



OPEN

Intratumoral oncolytic herpes virus G47 Δ for residual or recurrent glioblastoma: a phase 2 trial

Tomoki Todo¹✉, Hirotaka Ito¹, Yasushi Ino¹, Hiroshi Ohtsu^{2,3}, Yasunori Ota⁴, Junji Shibahara⁵ and Minoru Tanaka¹

This investigator-initiated, phase 2, single-arm trial primarily assessed the efficacy of G47 Δ , a triple-mutated, third-generation oncolytic herpes simplex virus type 1, in 19 adult patients with residual or recurrent, supratentorial glioblastoma after radiation therapy and temozolomide (UMIN-CTR Clinical Trial Registry UMIN000015995). G47 Δ was administered intratumorally and repeatedly for up to six doses. The primary endpoint of 1-yr survival rate after G47 Δ initiation was 84.2% (95% confidence interval, 60.4–96.6; 16 of 19). The prespecified endpoint was met and the trial was terminated early. Regarding secondary endpoints, the median overall survival was 20.2 (16.8–23.6) months after G47 Δ initiation and 28.8 (20.1–37.5) months from the initial surgery. The most common G47 Δ -related adverse event was fever (17 of 19) followed by vomiting, nausea, lymphocytopenia and leukopenia. On magnetic resonance imaging, enlargement of and contrast-enhancement clearing within the target lesion repeatedly occurred after each G47 Δ administration, which was characteristic to this therapy. Thus, the best overall response in 2 yr was partial response in one patient and stable disease in 18 patients. Biopsies revealed increasing numbers of tumor-infiltrating CD4⁺/CD8⁺ lymphocytes and persistent low numbers of Foxp3⁺ cells. This study showed a survival benefit and good safety profile, which led to the approval of G47 Δ as the first oncolytic virus product in Japan.

Glioblastoma has a poor prognosis with a median overall survival (OS) of 20.9 months despite the current Stupp regimen of radiotherapy plus temozolomide together with tumor-treating fields (TTF)¹. This regimen with TTF is the current standard-of-care for newly diagnosed glioblastoma in the United States, but its recommendation level as a standard-of-care varies among countries outside the United States. None of the current therapies can yet prevent recurrence of glioblastoma, not to mention cure it, so nonconventional therapeutic approaches are needed especially for recurrent cases.

G47 Δ is a triple-mutated, third-generation oncolytic herpes simplex virus type 1 (HSV-1) constructed by deleting the $\alpha 47$ gene and overlapping *US11* promoter from parental G207, a second-generation oncolytic HSV-1 with deletions in both copies of the $\gamma 34.5$ gene and an inactivation of the *ICP6* gene². G47 Δ shows greater tumor-specific replication capability and cytopathic effects than G207 but retains a high safety profile^{3,4}. G47 Δ was confirmed safe in the first-in-human (FIH) trial when administered intratumorally, two doses within 2 weeks, to patients with recurrent glioblastoma⁵. Preclinical studies show that G47 Δ exhibits efficacy via two mechanisms: (1) an immediate effect via virus replication and direct oncolytic activity; and (2) a delayed effect via induction of specific antitumor immunity².

In Japan, national health insurance allows patients to choose any government-approved treatment at any institution and at relatively low cost⁶. In clinical studies for lethal diseases in Japan, setting a noncurable standard-care control arm would not be accepted and also would be unethical, especially if the study was an academia-initiated, research grant-supported drug development such as this. Further, because G47 Δ needs to be administered by surgery, blinding treatment arms and allowing sham surgery on

randomly selected patients would not be considered acceptable in Japan.

This phase 2 trial is, therefore, designed as a single-arm trial to evaluate the efficacy of G47 Δ in patients with glioblastoma that was residual or recurred after initial therapy of surgery, radiation and temozolomide.

Results

The interim analysis in 13 patients showed a 1-yr survival rate after G47 Δ initiation of 92.3% (95% confidence interval (95% CI), 64.0–99.8). Compared with the preset control value of 15%, the O'Brien–Fleming boundary was crossed for the planned interim report ($Z_0 = 7.806$). This confirmed that the prespecified primary endpoint of this study was met and, therefore, the trial was terminated early by the recommendation of the Independent Data Monitoring Committee and as predetermined by the protocol. Of 28 patients who gave informed consent, 19 patients who matched the eligibility criteria had been enrolled and composed the full analysis set (FAS) (Extended Data Fig. 1). Demographics and baseline clinical characteristics of these 19 enrolled patients are shown in Table 1.

Magnetic resonance imaging (MRI)-guided stereotactic injection. A total of 97 stereotactic surgeries were performed in 19 enrolled patients. Twelve patients (63.2%) received G47 Δ administration the maximum of six times (Table 2). For the others, G47 Δ treatment was discontinued for meeting one of the treatment discontinuation criteria, as follows: progressive disease judgment by increase in target lesion size ($n = 3$), aggravation of symptoms ($n = 2$), clinical judgment by investigator (postoperative infection) ($n = 1$) and shrinkage of the target lesion to <1 cm in diameter ($n = 1$).

¹Division of Innovative Cancer Therapy, Advanced Clinical Research Center, and Department of Surgical Neuro-Oncology, The Institute of Medical Science, The University of Tokyo, Tokyo, Japan. ²Department of Data Science, National Center for Global Health and Medicine in Japan, Tokyo, Japan. ³Leading Center for the Development and Research of Cancer Medicine, Juntendo University, Tokyo, Japan. ⁴Department of Pathology, The Institute of Medical Science, The University of Tokyo, Tokyo, Japan. ⁵Department of Pathology, Kyorin University School of Medicine, Tokyo, Japan. ✉e-mail: toudou-nsu@umin.ac.jp

Table 1 | Baseline demographic and clinical characteristics

Pt no.	Sex/age	KPS	Tumor location	Surgery	Radiation (Gy/fr)	Chemotherapy other than TMZ	HSV-1 IgM/IgG ^a	Ki-67 (%)	IDH1	MGMT promoter MSP	MGMT expression	Rec/Res	Time from initial surgery to G47Δ (months)	Tumor area Baseline (mm ²)	MET-PET L/N	Steroids Before G47Δ	New or increased dose during G47Δ treatment
1	M/54	90	R/Fr	GTR	50.4/28	–	0.23/<2.0	4	wt	NA	+	1st	12.4	375.2	1.71	–	–
2	M/49	90	R/Fr	PR	60/30	–	0.09/<2.0	5	wt	NA	–	Res	3.0	220.0	1.50	–	–
3	F/63	80	L/Fr	PR	60/30	–	0.10/15.1	5	wt	NA	+	Res	3.4	661.4	3.62	–	–
4	M/69	90	L/T	GTR	60/30	–	0.19/2.7	15	wt	unmet	+	1st	8.7	176.9	1.78	–	–
5	M/46	100	R/Fr	GTR	50.4/28	BEV	0.46/51.4	6	wt	unmet	–	1st	14.1	554.2	1.95	–	Hydrocortisone (500 mg x1 dose, 5 times)
6	F/25	70	L/P	PR	60/30	BEV, BCNU wafer	0.13/<2.0	7	mt	unmet	+	2nd	23.5	696.6	2.15	–	–
7	M/51	90	R/T	PR	60/30	–	0.44/<2.0	40	wt	NA	–	Res	3.0	440.7	2.50	–	–
8	M/73	70	R/Fr	PR	60/30	–	0.18/123.0	30	wt	NA	+	1st	5.3	1,386.5	1.02	Prednisolone 10 mg d ⁻¹	–
9	M/46	100	R/Fr	GTR	60/30	BCNU wafer, IFNβ	0.18/<2.0	8	wt	NA	–	1st	24.9	122.4	1 ^b	–	–
10	M/28	100	L/Fr	GTR	60/30	BEV, BCNU wafer	0.24/<2.0	30–40	mt	NA	–	1st	9.4	141.4	1.60	–	–
11	M/53	80	R/T	GTR	60/30	BCNU wafer	0.20/<2.0	2	mt	NA	–	1st	7.4	416.2	1.35	–	–
12	M/59	70	L/Fr	Biopsy	60/30	BEV	0.31/2.3	40	wt	met	–	1st	4.2	519.9	1.38	–	Dexamethasone (19.8 mg d ⁻¹ to 6.6 mg d ⁻¹ x6 d, 1 time)
13	F/53	70	R/Fr	PR	60/30	BEV, BCNU wafer	0.45/105.0	30	mt	met	–	Res	4.1	873.1	1.86	–	–
14	M/42	80	Splenium	PR	60/30	–	0.19/<2.0	50	wt	NA	+	1st	10.1	1,832.2	2.27	–	Dexamethasone (19.8 mg d ⁻¹ to 13.2 mg d ⁻¹ x4 d, 1 time); prednisolone (30 mg d ⁻¹ to 15 mg d ⁻¹ x6 d, 1 time)
15	M/65	80	L/P	Biopsy	60/30	BEV	0.23/164.0	15	wt	NA	+	Res	4.4	652.8	1.54	–	Betamethasone (24 mg d ⁻¹ to 6 mg d ⁻¹ x6 d, 1 time)
16	M/45	100	R/Fr	PR	60/30	BCNU wafer	0.10/<2.0	50	mt	NA	–	Res	3.1	2,306.7	2.64	–	–
17	M/68	90	R/T	PR	60/30	–	0.18/220.0	20	wt	NA	+	Res	3.9	291.5	2.39	–	–
18	F/43	80	L/P	Biopsy	60/30	BEV	0.30/216.0	10	wt	NA	–	Res	3.8	513.5	2.01	–	Prednisolone (30 mg d ⁻¹ x7 d, 1 time)
19	M/35	80	R/Fr	PR	59.4/33	–	0.14/<2.0	90	mt	NA	–	Res	3.6	778.5	1.27	–	–

Abbreviations: F, female; M, male; KPS, Karnofsky Performance Scale; R, right; L, left; Fr, frontal lobe; T, temporal lobe; P, parietal lobe; GTR, gross total resection; PR, partial resection; TMZ, temozolomide; BEV, bevacizumab; BCNU wafer, carmustine wafer; IFNβ, interferon-β; HSV-1, herpes simplex virus type 1; IDH1, isocitrate dehydrogenase 1; mt, mutant type; wt, wild type; MGMT, methylguanine methyltransferase; MSP, methylation-specific PCR; met, methylated; unmet, unmethylated; NA, not available; Rec, recurrent; Res, residual; 1st, first recurrence; 2nd, second recurrence; MET, methionine; PET, positron emission tomography; L/N, lesion-to-normal ratio; ^a1 d before first therapy; ^bL/N could not be measured, because there was no increased uptake corresponding to the target lesion. GTR is defined as >95% of the tumor removed assessed by the surgeon. Resection other than GTR is either PR or biopsy as judged by the surgeon. Immunohistochemistry for MGMT expression: –, <10%; +, ≥10% and <50%; ++, ≥50%.

Table 2 | Summary of patient outcomes

Patient no.	Sex/age	Number of G47Δ doses	Time to progression (d) ^a	Best response	OS (d)		Treatment after progression	Outcome	Autopsy	Cause of death
					After initial surgery	After 1st G47Δ therapy				
1	M/54	6	258	SD	863	485	Bevacizumab after reoperation (GTR)	Dead	+	Tumor progression
2	M/49	6	588	SD	1,748	1,657	Extended field SRS	Dead	+	Tumor progression
3	F/63	6	762 ^b	SD	1,044	941	–	Dead	–	Tumor progression
4	M/69	5	115	SD	891	626	Bevacizumab	Dead	–	Tumor progression
5	M/46	6	133	SD	1,310	882	Bevacizumab after reoperation (GTR) Nimustine	Dead	+	Tumor progression
6	F/25	3	43	SD	897	181	Bevacizumab	Dead	–	Tumor progression
7	M/51	2	64	SD	489	398	Bevacizumab	Dead	–	Tumor progression
8	M/73	6	294	SD	817	655	Extended field SRS; bevacizumab	Dead	–	Tumor progression
9	M/46	6	1,696 ^b	SD	2,716 ^c	1,960 ^c	–	Stable	NA	NA
10	M/28	4	79	SD	1,452	1,166	Extended field SRS	Dead	–	Tumor progression
11	M/53	6	1,584 ^b	SD	2,073 ^c	1,848 ^c	–	Stable	NA	NA
12	M/59	6	139	SD	596	469	Bevacizumab	Dead	–	Tumor progression
13	F/53	6	573 ^b	SD	709	583	–	Dead	+	Not related to the disease
14	M/42	4	78	SD	543	236	Bevacizumab	Dead	–	Tumor progression
15	M/65	6	142	SD	569	434	Bevacizumab	Dead	–	Tumor progression
16	M/45	6	163	SD	699	606	Extended field SRS; bevacizumab	Dead	+	Tumor progression
17	M/68	2	127	PR	1,554 ^c	1,435 ^c	Bevacizumab after reoperation (partial resection)	Stable	NA	NA
18	F/43	5	108	SD	244	127	–	Dead	–	Tumor progression
19	M/35	6	331	SD	667	556	Bevacizumab; spinal irradiation	Dead	–	Tumor progression

Abbreviations: F, female; M, male; PR, partial response; SD, stable disease; GTR, gross total resection; SRS, stereotactic radiosurgery (radiotherapy). ^aIncluding the date of first administration. ^bTumor progression occurred after initial cut-off date for judgment of outcome. ^cPatient remained alive at most recent observation date (1 March 2022) used to analyze survival. Extent of tumor resection at reoperation: GTR is defined as >95% of the tumor removed assessed by the surgeon.

Efficacy. The primary endpoint was the 1-yr survival rate and the secondary endpoints included OS and progression-free survival (PFS), all after G47Δ initiation. For the FAS population, the 1-yr survival rate after G47Δ initiation was 84.2% (95% CI, 60.4–96.6). The median OS was 20.2 (16.8–23.6) months after G47Δ initiation (Fig. 1a and Table 2), and the median PFS was 4.7 (3.3–6.1) months after G47Δ initiation (Fig. 1b). As an exploratory endpoint, the Kaplan–Meier curve for OS from the initial surgery (initial diagnosis) showed a median OS of 28.8 (20.1–37.5) months (Extended Data Fig. 2a).

Because the action of G47Δ does not theoretically depend on the genetic background of tumor cells, and testing for isocitrate dehydrogenase 1 (IDH1) mutation was not regularly performed in 2014 when this trial protocol was submitted to the Japanese Pharmaceuticals and Medical Devices Agency (PMDA), the status of IDH1 mutation was not included as a covariate of this study. However, all 19 patients were examined post hoc with regard to the IDH1 status, and IDH1

mutation was found in 6 of 19 patients (Table 1). Kaplan–Meier analysis showed that median OS after G47Δ initiation was not affected by IDH1 status (wild type, 20.9 (13.6–28.2) months; mutant type, 19.4 (17.4–21.4) months; $P=0.899$, log-rank test) (Fig. 1c). Kaplan–Meier analysis also showed that median OS from the initial surgery was not affected by IDH1 status (wild type, 28.8 (17.6–40.0) months; mutant type, 23.6 (16.1–31.1) months; $P=0.769$, log-rank test; Extended Data Fig. 2b).

MGMT methylation status was available for five patients (26.3%) from referring hospitals; three were unmethylated and two were methylated (Table 1). The paraffin-embedded slide sections of initial surgery provided from referring hospitals and the biopsy specimens from this trial were not enough to extract sufficient amounts of DNA to perform methylation-specific PCR. Alternatively, we performed immunohistochemistry for the expression of MGMT using the provided paraffin-embedded slide sections post hoc. MGMT immunohistochemistry was negative (–) in 11 of 19

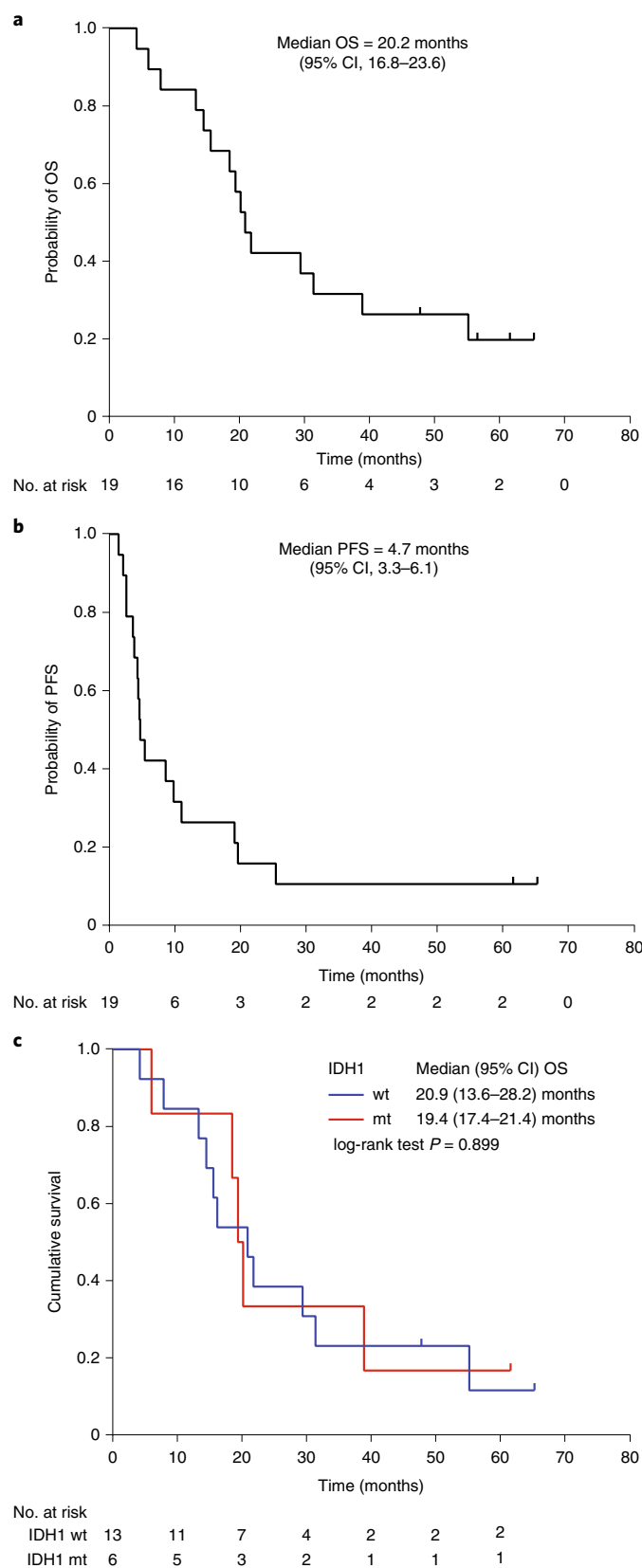


Fig. 1 | Kaplan-Meier curves after G47Δ initiation. a–c, Kaplan-Meier curves for OS after G47Δ initiation (**a**), PFS after G47Δ initiation (**b**) and OS based on IDH1 status after G47Δ initiation (**c**). The data were analyzed and Kaplan-Meier curves created on 1 March 2022.

patients (57.9%), positive (+) in 8 of 19 (42.1%) and strongly positive (++) in none (Table 1). Kaplan–Meier analyses showed that median OS was not affected by MGMT expression, both after G47Δ initiation (MGMT–, 20.2 (8.4–32.0) months; MGMT+, 16.2 (7.3–25.1) months; $P=0.428$, log-rank test) and from the initial surgery (MGMT–, 23.6 (0.4–46.8) months; MGMT+, 28.8 (25.3–32.3) months; $P=0.621$, log-rank test) (Extended Data Fig. 3).

As one of the secondary endpoints, the best overall response between the first G47Δ administration and 24 months after the last administration was PR in 1 patient (5.3%) and stable disease in 18 patients (94.7%). The discrepancy between the survival benefit and the tumor response assessed on MRI is likely characteristic to G47Δ treatment. The low response rate was as expected, because the target lesion typically enlarges after G47Δ administration and maintains the size for a certain duration as described below.

The time course of cross-sectional area of the target lesion of each patient on MRI without bevacizumab treatment is shown in Extended Data Fig. 4. The reduction in target lesion areas observed in some patients at later time points was not associated with corticosteroid administration. Three patients (no. 6, no. 14, no. 18) died within 1 yr of G47Δ therapy (<1-yr group), whereas five patients (no. 2, no. 9, no. 10, no. 11, no. 17) survived longer than 3 yr after G47Δ therapy (>3-yr group; Table 2). The mean tumor area (\pm s.d.) at the initiation of G47Δ therapy of the <1-yr group and that of the >3-yr group were $1,014.1 \pm 714.4$ mm² and 238.3 ± 120.0 mm², respectively, indicating that patients who survived >3 yr had significantly smaller initial tumor sizes than those who survived <1 yr ($P=0.036$, Mann–Whitney U -test).

Safety. Safety was one of the secondary endpoints. For the total study population, 19 patients (100.0%) experienced G47Δ-related adverse events (Table 3). The major G47Δ-related adverse events included fever (89.5%), vomiting (57.9%), nausea (52.6%), lymphocyte count decrease (47.4%) and white blood cell decrease (31.6%). The G47Δ-related grade ≥ 3 adverse event of lymphocyte count decrease occurred in five patients (26.3%), but all recovered without any treatment. The only serious adverse event attributable to G47Δ was fever (grade 2) in one patient (5.3%) that caused a prolongation of hospitalization. Overall adverse events are summarized in Supplementary Table 1. A grade 5 event occurred in one patient who died in the bath 15 months after the last G47Δ administration. Autopsy revealed that the lesion was well controlled and the death ‘not related’ to G47Δ.

Viral shedding. The viral shedding study was an exploratory endpoint. Blood, urine and saliva samples were collected at designated time points as described in the Methods. G47Δ DNA was detected from the blood of patient no. 4 on day 0 only. All other samples were negative by quantitative PCR.

Imaging. MRI analyses were an exploratory endpoint. Two MRI features commonly observed in all patients in the FIH trial were also observed in this phase 2 trial: (1) clearing of contrast-enhancement at the injection site; and (2) mild enlargement of target lesions (Fig. 2a). This was observed immediately after G47Δ administration and occurred repeatedly after every G47Δ administration for up to six doses. As G47Δ was administered to a different coordinate for each injection and at two sites within the tumor for each dose (Fig. 2b and Extended Data Fig. 5), the area of clearing typically increased as the doses increased, leading to a large hollow within the target lesion with an increase in diameter after repeated G47Δ doses, mimicking aerial bombing of a surrounded field (Fig. 2a). These MRI changes generally ceased once G47Δ administration was terminated, and the target lesion stayed stable until tumor regrowth (Fig. 2a).

Table 3 | Treatment-emergent adverse events attributable to G47Δ according to severity grade, n = 19

Body system and adverse event, n (%)	Grade 1	Grade 2	Grade 3	Grade 4	Grade 5
Patient number with any adverse event	2 (10.5)	10 (52.6)	5 (26.3)	2 (10.5)	
General disorder					
Fever	6 (31.6)	10 (52.6)	1 (5.3)	0 (0)	0 (0)
Gastrointestinal disorder					
Vomiting	3 (15.8)	7 (36.8)	1 (5.3)	0 (0)	0 (0)
Nausea	5 (26.3)	5 (26.3)	0 (0)	0 (0)	0 (0)
Nervous system disorder					
Seizure	0 (0)	3 (15.8)	0 (0)	0 (0)	0 (0)
Cerebral edema	2 (10.5)	1 (5.3)	0 (0)	0 (0)	0 (0)
Neuropathy-sensory	1 (5.3)	0 (0)	0 (0)	0 (0)	0 (0)
Headache	1 (5.3)	0 (0)	0 (0)	0 (0)	0 (0)
Blood					
Anemia	1 (5.3)	0 (0)	0 (0)	0 (0)	0 (0)
Investigations					
Lymphocyte count decreased	1 (5.3)	3 (15.8)	3 (15.8)	2 (10.5)	0 (0)
White blood cell count decreased	2 (10.5)	3 (15.8)	1 (5.3)	0 (0)	0 (0)
Neutrophil count decreased	0 (0)	2 (10.5)	1 (5.3)	0 (0)	0 (0)
Platelet count decreased	3 (15.8)	0 (0)	0 (0)	0 (0)	0 (0)
Bilirubin increased	1 (5.3)	0 (0)	0 (0)	0 (0)	0 (0)
γ-Glutamyl transpeptidase increased	1 (5.3)	0 (0)	0 (0)	0 (0)	0 (0)
PT-INR increased	1 (5.3)	0 (0)	0 (0)	0 (0)	0 (0)
Hypoalbuminemia	1 (5.3)	0 (0)	0 (0)	0 (0)	0 (0)
Hyponatremia	1 (5.3)	0 (0)	0 (0)	0 (0)	0 (0)

CTCAE v.4.03 Japanese version was used to determine each grade. PT-INR, prothrombin time-international normalized ratio.

We also observed that target lesions were relatively well controlled after G47Δ therapy. However, at progression, we often observed remote new lesions (Fig. 3a), intrathecal dissemination (Extended Data Fig. 6) and tumor extension to sites adjacent to but away from the target lesion (Extended Data Fig. 7).

Long-term efficacy, supposedly via antitumor immunity, was observed in patient no. 10 (Fig. 3). This patient was judged as having progressive disease due to the appearance of a remote new lesion, so G47Δ therapy was terminated after four administrations. However, the new lesion disappeared after 1 month, followed by eventual shrinkage of the target lesion.

Histology. The histology study was an exploratory endpoint. Biopsies were performed immediately before each G47Δ injection. All patients were confirmed to have viable glioblastoma in at least one of the biopsies. Biopsies also confirmed that all recurrent cases were not pseudoprogression. As G47Δ was injected to different coordinates, biopsy results reflected the histopathology distant from previous G47Δ injections. The histology was characterized by: (1) infiltration of CD4⁺ and CD8⁺ lymphocytes within the tumor that increased abundantly in number as G47Δ injections were repeated; and (2) a low number of Foxp3⁺ cells that remained so despite repeated G47Δ injections (Figs. 2c and 3b and Supplementary Fig. 1). In one patient who showed tumor regrowth 4 months after G47Δ therapy, the high numbers of CD4⁺ and CD8⁺ lymphocytes persisted whereas the number of Foxp3⁺ cells increased (Fig. 2d). Histology results of regrown tumors at reoperation and brain lesions at autopsy are described in Extended Data Fig. 8.

Treatment after G47Δ. Of 15 patients who experienced disease progression after G47Δ, 9 patients received bevacizumab

every 4 weeks, 3 patients received bevacizumab after reoperation and 4 patients received extended field stereotactic radiotherapy (Table 2)⁷. One patient with a temozolomide allergy received nimustine as second-line therapy. Sixteen patients received steroids (dexamethasone at mean dose of 13.2 mg × 6 d) after symptomatic progression. At the time of writing, 16 of 19 patients had died with 5 patients having undergone autopsy.

Discussion

This trial demonstrates the efficacy and safety of G47Δ for residual or recurrent glioblastoma. The 1-yr survival rate of 84.2% and the median OS and PFS of 20.2 months and 4.7 months, respectively, after G47Δ initiation compare favorably with other treatments. Pooled data from 16 trials of various chemotherapy agents for treating recurrent glioblastoma reported a median OS of 5.0 months and a median PFS of 1.8 months (ref. ⁸). Median OS of 6.6 months and 5.3 months are reported for temozolomide monotherapy rechallenge in patients with recurrent glioblastoma receiving adjuvant temozolomide and after a temozolomide-free interval, respectively⁹. A phase 2 study using bevacizumab reported a median OS of 9.2 months in recurrent glioblastoma¹⁰. Immune checkpoint inhibitors and various molecule-targeted therapies have not shown improved efficacy for recurrent glioblastoma, with median OS of 4.4–9.9 months (refs. ^{11,12}). In patients with newly diagnosed glioblastoma, a randomized trial showed a median OS of 20.9 months for the TTF-temozolomide group versus 16.0 months in the temozolomide-alone group¹. However, in patients with recurrent glioblastoma, TTF failed to provide significant survival advantage over chemotherapy (median OS 6.6 versus 6.0 months)¹³. In this G47Δ phase 2 trial, the median OS was 28.8 months from the initial surgery.

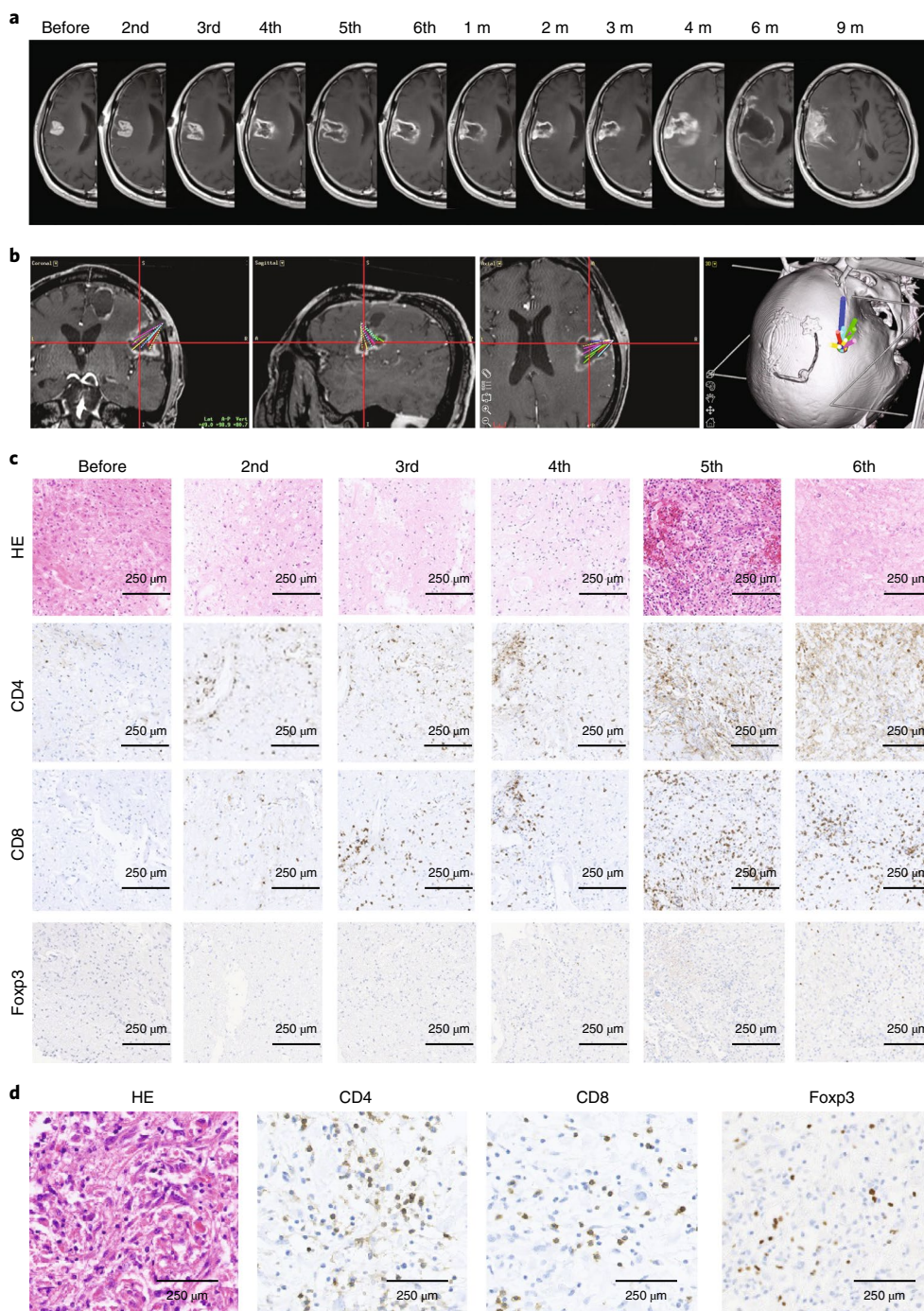


Fig. 2 | Representative case (patient no. 1) treated with G47 Δ . **a**, MRI images at indicated observation time points. Characteristic MRI changes were observed at every G47 Δ administration, that is, a clearing of contrast-enhancement at the injection site and an enlargement of the entire target lesion. G47 Δ was injected to different coordinates from previous injections, so the area of contrast-enhancement clearing increased as the doses increased, leading to a large hollow within the target lesion with an increase in diameter after six G47 Δ doses. The MRI changes ceased after the last G47 Δ injection and the target lesion stayed stable until 4 months after G47 Δ therapy, when the tumor showed a regrowth. The regrown tumor was resected at 6 months but further regrew at 9 months, and the patient died of exacerbation of the disease at 16.2 months after G47 Δ initiation. **b**, Planning MRI using StealthStation Surgical Navigation System at the 6th dose, displaying administration routes from the 2nd to 6th dose (10 injections) overlaid in the same image. **c**, Histology of biopsy specimens. Biopsies were performed before indicated injections and were obtained from coordinates different from previous G47 Δ injections. CD4⁺ and CD8⁺ lymphocytes infiltrating within the tumor increased abundantly in number as G47 Δ injections were repeated. In contrast, the number of tumor-infiltrating Foxp3⁺ cells remained low throughout repeated G47 Δ injections. Representative of four biopsy specimens. **d**, Histology of resected tumor at regrowth. The numbers of tumor-infiltrating CD4⁺ and CD8⁺ lymphocytes remained high in the regrown tumor resected 6 months after the last G47 Δ administration. A higher number of Foxp3⁺ cells are observed in the tumor at regrowth than in tumors during G47 Δ treatment. Representative of three tissue samples. HE, haematoxylin and eosin; m, month(s).

Since the status of IDH1 mutation was not included in the eligibility criteria, it was examined as a post hoc study, and 6 of 19 patients were found to be IDH1 mutated. However, the difference in IDH1 mutation was shown to have no impact on the OS both after G47 Δ initiation and from the initial surgery in this study. It has been reported that there is no difference in survival time after recurrence of glioblastoma with or without IDH mutation¹⁴. Six patients had carmustine (BCNU) wafers (Gliadel, Eisai, for Arbor Pharmaceuticals) placed in the tumor cavity at their initial surgeries, and it happened that five of six were IDH1 mutated. Although BCNU wafers (Gliadel) were reported effective for newly diagnosed malignant glioma, a survival benefit was not shown in the subset of patients with glioblastoma in a prospective, open-label, randomized trial¹⁵, and no significant survival benefit was found for glioblastoma even in the long-term follow-up of this trial¹⁶. Rather, it has been reported that the toxicity after Gliadel use is significantly higher, for patients with both newly diagnosed and recurrent glioblastoma¹⁷. The definition of glioblastoma was changed in the 2021 World Health Organization (WHO) classification, and glioblastoma in this study is a mixture of glioblastoma and grade 4 IDH-mutant astrocytoma according to the new WHO classification¹⁸.

The survival benefit without a remarkable tumor response on MRI is likely characteristic of G47 Δ therapy. The overall response rate was only 5.3%, with one PR case. Lymphocytes, presumably infiltrating towards tumor cells, accumulate within the tumor with repeated G47 Δ doses, so the actual antitumor effects are not reflected on image studies. This is quite opposite to the situation with bevacizumab, which shows excellent rates of radiographic response, but tumors continue to progress without survival benefits¹⁹. The presence of many cases that maintained stable disease in this phase 2 study was one of the factors of the drug approval by the PMDA.

Regarding the dosing schedule, G47 Δ was administered repeatedly for a maximum of six times. A preclinical study with G207 demonstrated that the efficacy of six intratumoral injections was superior to the efficacy of a single injection with a tenfold higher dose²⁰. The expected survival period of a patient with glioblastoma after recurrence is about 6 months with standard chemotherapy⁸. Furthermore, from an experienced neurosurgeon's perspective, repeating a burr hole surgery six times could be considered feasible without causing patients excessive suffering. Six doses are also acceptable cost wise for patients in Japan, because national health insurance covers the treatment during clinical trials and after drug approval, including surgery and in-patient care.

Adverse events related to G47 Δ were mostly restricted to those caused by immune responses and are likely consequences of the immune system attempting to eliminate an unnaturally large load of virus that robustly replicates in a localized area. As systemic responses, fever and headache were frequently manifested and, as a local response, tumor swelling was commonly observed. Fever and vomiting were the only two grade 3 adverse events attributable to G47 Δ and unrelated to blood cell counts. A similar adverse event profile, both systemic and local, has been noted with vaccines, such as the Pfizer-BioNTech COVID-19 vaccine²¹. Decreased lymphocyte count may be virus-related, but could not be distinguished from an adverse event caused by temozolomide²². Rationally, an effective countermeasure against immune responses is the use of corticosteroids²³. In the FIH study, we found that corticosteroid administration immediately diminished the immune response-related adverse events including fever and tumor swelling, and did not interfere with long-term antitumor immunity development when the duration was kept within 1 week (ref. 5). In this phase 2 study, corticosteroids were used in four patients (21.1%) to suppress G47 Δ adverse events, only once during the entire treatment in all cases. In contrast, a recombinant nonpathogenic polio-rhinovirus chimera (PVSRIPO) reportedly caused severe brain edema and neurologic

symptoms related to peritumoral inflammation when injected intratumorally in patients with glioblastoma, even causing death in one patient, and all patients required corticosteroid administration²⁴.

Dose-limiting toxicity has not been observed with G47 Δ . The concept of maximum tolerated dose being equivalent to the optimal dose in the development of chemotherapy drugs may not apply to oncolytic virus development. In fact, dose-limiting toxicity has not been observed with G207, the parental virus of G47 Δ , and the highest dose tested in the first phase 1 study was 3×10^9 plaque-forming units (p.f.u.) per dose²⁵, but lower doses, and not this highest dose, were used in the subsequent clinical trials^{26,27}. In practice, there are limits to the amount of virus per ml that can be manufactured, depending on the type of virus, and, in general, the higher the concentration, the higher the production cost when mass-produced under good manufacturing practices. Therefore, for practical realization of oncolytic virus therapy, it is also necessary to consider that the amount of oncolytic virus used to show efficacy can be manufactured as a product at a reasonable cost so that the price is affordable for patients after marketing.

At the time of this manuscript submission, three patients were alive and stable for more than 3 yr after the last G47 Δ administration. A proportion of G47 Δ -treated patients experienced long-term survival in this phase 2 study as well as in the FIH trial⁵. Such a proportion of long-term survival was similarly observed in the phase 1 trial of PVSRIPO in patients with glioblastoma²⁴. From in vivo replication studies in animals and biopsy specimens obtained from the exact coordinates of the first G47 Δ injection in the FIH trial⁵, we estimate that G47 Δ injected into glioblastoma is eliminated by the immune system within 4 weeks (refs. 2,28). Target lesions were generally well controlled. These facts indicate that a delayed effect of G47 Δ via induction of systemic antitumor immunity may be the major mechanism for long-term disease control.

To support the notion that specific antitumor immune responses are boosted after multiple G47 Δ injections, the biopsy histology revealed that tumor-infiltrating CD4⁺ and CD8⁺ lymphocyte populations increase with repeated G47 Δ injections. These lymphocytes which recognize and infiltrate towards tumor cells appear almost immediately after G47 Δ therapy. However, it takes approximately 4 months or more after initiation of G47 Δ therapy until the antitumor immunity causes tumor shrinkage, although it may be acting from much earlier to suppress tumor growth. Therefore, lymphocytes that rapidly infiltrate the tumor may recognize the tumor cells but their exact functions are yet to be elucidated. Tumor-infiltrating CD4⁺ and CD8⁺ lymphocytes persisted for a long time (>50 months), as observed in resected regrown tumors and at autopsies. Cells with Foxp3, which acts as a master transcription factor for regulatory T cells²⁹, were rarely found in biopsy specimens despite repeated G47 Δ injections. Since an increased number of Foxp3⁺ cells were observed in some of the tumors that regrew after G47 Δ therapy, inhibition of Foxp3⁺ cells may be relevant to G47 Δ efficacy. We also observed that lesions close to G47 Δ injection sites were relatively well controlled, although tumor regrowth was often observed remote from the target lesion or as dissemination via cerebrospinal fluid. Interestingly, in a phase 3 trial of the oncolytic HSV-1 talimogene laherparepvec (T-Vec), patients with stage IIIB-IVM1c melanoma also experienced more frequent immune-related antitumor effects on nontreated lesions close to treated lesions than distant ones³⁰. The common observation with G47 Δ in the brain and T-Vec outside the brain, that nontreated lesions close to the treated lesion are better controlled than distant ones, suggests the presence of action mechanisms of antitumor immunity that are not yet known.

The characteristic MRI changes were observed after every G47 Δ injection regardless of repeated administration. The biopsy histology of the FIH trial revealed that clearing at the injection site reflected the area of virus replication and tumor cell destruction⁵. This study further demonstrates that the immediate enlargement

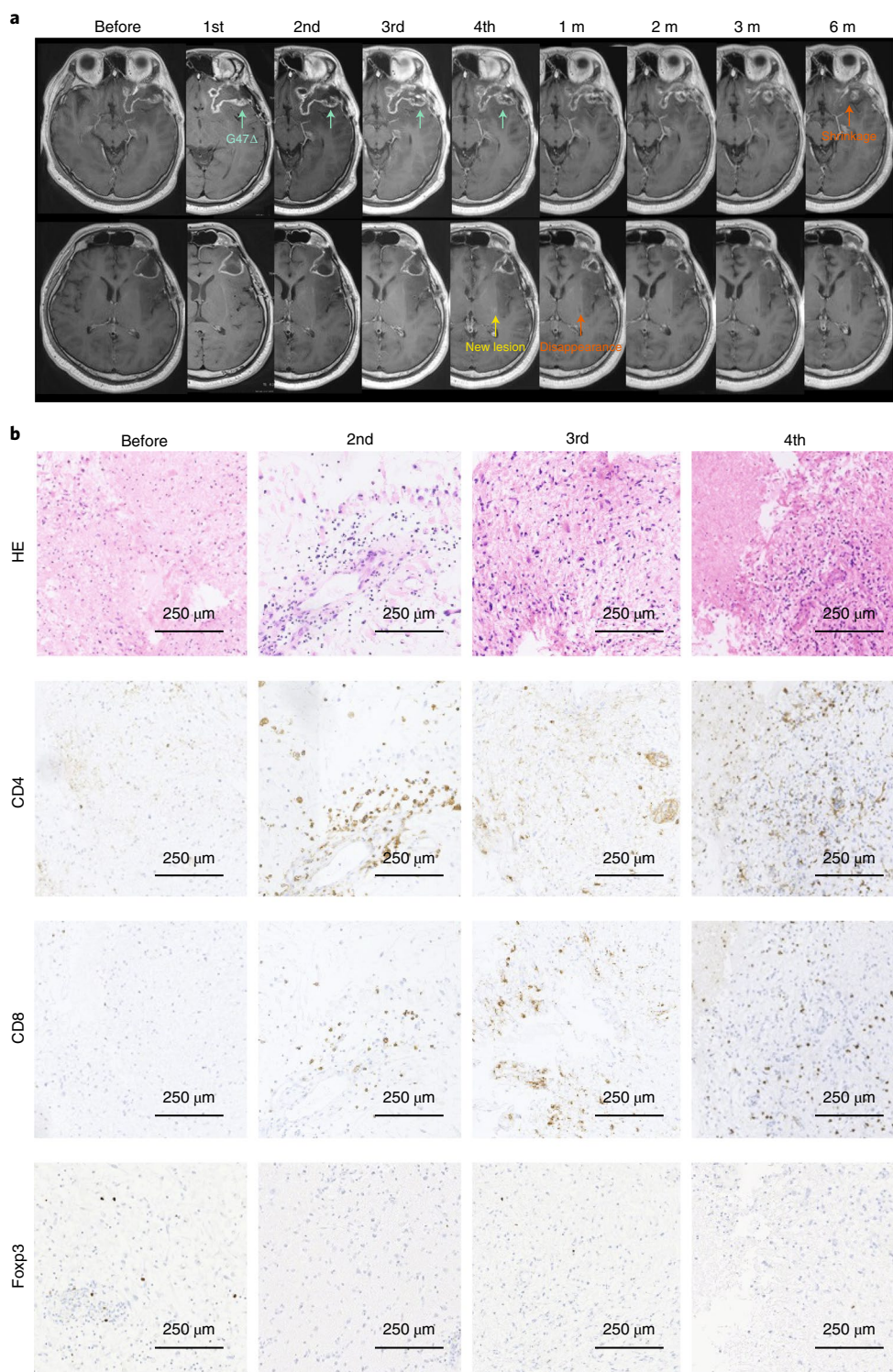


Fig. 3 | Representative case (patient no. 10) showing a long-term efficacy via antitumor immunity. a, MRI images at indicated observation time points. G47 Δ was injected into the target lesion (green arrows), causing the characteristic appearance of contrast-enhancement clearing at the injection site and an enlargement of the entire target lesion. After four doses, a new lesion (yellow arrow) appeared in the left basal ganglia remote from the target lesion, so G47 Δ therapy was terminated. However, at the first follow-up 1 month after the last G47 Δ administration, the new lesion disappeared (orange arrow at 1 month). Eventually, in the observations that followed, the target lesion decreased in size (orange arrow at 6 months). Remote new lesions further appeared at 24 months and the patient died of exacerbation of the disease at 38.9 months after G47 Δ initiation. **b,** Histology of biopsy specimens. Biopsies were performed before indicated injections and were obtained from coordinates different from previous G47 Δ injections. Similar to patient no. 1, CD4⁺ and CD8⁺ lymphocytes infiltrating within the tumor increased abundantly in number as G47 Δ injections were repeated, whereas the number of tumor-infiltrating Foxp3⁺ cells remained low throughout repeated G47 Δ injections.

of the target lesion is caused by rapid infiltration of lymphocytes within the tumor, which may be called ‘immunoprogession’ and should be clearly distinguished from pseudoprogession that occurs after radiation therapy. Although it has been reported that angiogenesis is stimulated by G47Δ in a mouse model³¹, the enlargement of the target lesion occurs immediately and every time after G47Δ injection, so rapid lymphocyte infiltration is more likely the contributing mechanism than angiogenesis.

The response criteria adopted in this trial functioned well, and 12 patients (63.2%) were able to receive a total of 6 doses without being prematurely judged to have tumor progression. Of these 12 patients, 7 patients showed a reduction in target lesion size after a temporary increase, typically 9–12 months after the last G47Δ dose. Since G47Δ replication supposedly ceases much earlier, such shrinkage of the target lesion is likely due to a delayed effect of G47Δ via elicited antitumor immunity. In addition, patients that survived >3 yr after G47Δ therapy had smaller initial tumor sizes than those that survived <1 yr. Thus, G47Δ treatment earlier in the course of this disease may be warranted to achieve high efficacy and potentially obtain a cure. One patient from this trial and one patient from the FIH trial showed long-term survival, with lesions controlled after only two G47Δ administrations, so the number of administrations required for an effective response apparently varies among individuals. An adequate frequency of G47Δ injections is expected to become clear in a planned post-marketing investigation.

G47Δ represents an evolved oncolytic virus clinically tested for gliomas that include Newcastle disease virus, reovirus, parvovirus, adenovirus, polio virus and vaccinia virus³². PVSRIPO, a recombinant poliovirus-rhinovirus chimera mentioned earlier, has shown efficacy in a single phase I clinical trial of 61 patients, although the improvement in median OS was modest²⁴. Among adenovirus candidates, DNX-2401 has shown evidence of viral-induced necrosis in patients with malignant glioma and has been fast-tracked as an orphan drug by the US Food and Drug Administration³³. G207 was recently shown to be safe in children with supratentorial high-grade glioma³⁴.

During this phase 2 trial, G47Δ was designated as a SAKIGAKE (breakthrough therapy) Product, and further as an Orphan Regenerative Medicine Product for malignant glioma by the Japanese Ministry of Health, Labor and Welfare (MHLW), allowing fast-track review and approval. Hence, this phase 2 trial served as a pivotal study, and led to the conditional and time-limited approval of G47Δ for malignant glioma by the MHLW on 11 June 2021 as a Gene Therapy Product, the first oncolytic virus drug in Japan (https://www.daiichisankyo.com/files/news/pressrelease/pdf/202106/20210611_E_47.pdf; DELYTACT oncolytic virus G47Δ approved in Japan for treatment of patients with malignant glioma). The study population was rather small, with 97 surgeries in 19 patients, one factor for which was that this was an academia-initiated drug development for rare cancer in the Japanese medical system under Japanese regulations for gene therapy. It is planned that all patients using commercially distributed G47Δ be registered and followed, and clinical data evaluated against a control population of patients under PMDA supervision in the next 7 yr. G47Δ is perhaps the first new drug since temozolomide and the first new treatment since TTF that shows a survival benefit for glioblastoma, and provides a potential cure in a proportion of patients. Now that this nonconventional therapeutic modality is approved as a treatment option in Japan, the standard care of malignant glioma may change in the future.

To date, G47Δ has been shown to be efficacious via the same mechanism of action in various solid tumors in vivo, including prostate cancer, gastric cancer, hepatocellular carcinoma, tongue cancer, esophageal cancer, breast cancer, neuroblastoma and malignant peripheral nerve sheath tumor^{2,3,35–41}. Oncolytic HSV-1, including G47Δ, does not infect normal bone marrow-derived cells^{2,42}, but recent studies show that even some blood cancers are

susceptible to G47Δ (refs. ^{43,44}). Further, G47Δ has been shown to have augmented efficacy when used in combination with immune checkpoint inhibitors^{38,45,46}. We will pursue expansion of indications for G47Δ to other solid cancers as swiftly as possible.

Online content

Any methods, additional references, Nature Research reporting summaries, source data, extended data, supplementary information, acknowledgements, peer review information; details of author contributions and competing interests; and statements of data and code availability are available at <https://doi.org/10.1038/s41591-022-01897-x>.

Received: 16 January 2022; Accepted: 9 June 2022;

Published online: 21 July 2022

References

- Stupp, R. et al. Effect of tumor-treating fields plus maintenance temozolomide vs maintenance temozolomide alone on survival in patients with glioblastoma: a randomized clinical trial. *JAMA* **318**, 2306–2316 (2017).
- Todo, T., Martuza, R. L., Rabkin, S. D. & Johnson, P. A. Oncolytic herpes simplex virus vector with enhanced MHC class I presentation and tumor cell killing. *Proc. Natl Acad. Sci. USA* **98**, 6396–6401 (2001).
- Ma, W., He, H. & Wang, H. Oncolytic herpes simplex virus and immunotherapy. *BMC Immunol.* **19**, 40 (2018).
- Carson, J., Haddad, D., Bressman, M. & Fong, Y. Oncolytic herpes simplex virus 1 (HSV-1) vectors: increasing treatment efficacy and range through strategic virus design. *Drugs Future* **35**, 183–195 (2010).
- Todo, T., Ino, Y., Ohtsu, H., Shibahara, J. & Tanaka, M. A phase I/II study of triple-mutated oncolytic herpes virus G47Δ in patients with progressive glioblastoma. *Nature Commun.* (in the press).
- Ikegami, N. et al. Japanese universal health coverage: evolution, achievements, and challenges. *Lancet* **378**, 1106–1115 (2011).
- Koga, T. et al. Extended field stereotactic radiosurgery for recurrent glioblastoma. *Cancer* **118**, 4193–4200 (2012).
- Ballman, K. V. et al. The relationship between six-month progression-free survival and 12-month overall survival end points for phase II trials in patients with glioblastoma multiforme. *Neuro Oncol.* **9**, 29–38 (2007).
- Wick, A. et al. Rechallenge with temozolomide in patients with recurrent gliomas. *J. Neurol.* **256**, 734–741 (2009).
- Friedman, H. S. et al. Bevacizumab alone and in combination with irinotecan in recurrent glioblastoma. *J. Clin. Oncol.* **27**, 4733–4740 (2009).
- Roy, S., Lahiri, D., Maji, T. & Biswas, J. Recurrent glioblastoma: where we stand. *South Asian J. Cancer* **4**, 163–173 (2015).
- Brahm, C. G. et al. The current status of immune checkpoint inhibitors in neuro-oncology: a systematic review. *Cancers (Basel)* **12**, 586 (2020).
- Stupp, R. et al. NovoTTF-100A versus physician's choice chemotherapy in recurrent glioblastoma: a randomised phase III trial of a novel treatment modality. *Eur. J. Cancer* **48**, 2192–2202 (2012).
- Mandel, J. J. et al. Impact of IDH1 mutation status on outcome in clinical trials for recurrent glioblastoma. *J. Neurooncol.* **129**, 147–154 (2016).
- Westphal, M. et al. A phase 3 trial of local chemotherapy with biodegradable carmustine (BCNU) wafers (Gliadel wafers) in patients with primary malignant glioma. *Neuro Oncol.* **5**, 79–88 (2003).
- Westphal, M., Ram, Z., Riddle, V., Hilt, D. & Bortey, E. Gliadel wafer in initial surgery for malignant glioma: long-term follow-up of a multicenter controlled trial. *Acta Neurochir. (Wien)* **148**, 269–275; discussion 275 (2006).
- De Bonis, P. et al. Safety and efficacy of Gliadel wafers for newly diagnosed and recurrent glioblastoma. *Acta Neurochir. (Wien)* **154**, 1371–1378 (2012).
- Louis, D. N. et al. The 2021 WHO Classification of Tumors of the Central Nervous System: a summary. *Neuro Oncol.* **23**, 1231–1251 (2021).
- Li, Y., Ali, S., Clarke, J. & Cha, S. Bevacizumab in recurrent glioma: patterns of treatment failure and implications. *Brain Tumor Res. Treat.* **5**, 1–9 (2017).
- Chahlavi, A., Rabkin, S. D., Todo, T., Sundaresan, P. & Martuza, R. L. Effect of prior exposure to herpes simplex virus 1 on viral vector-mediated tumor therapy in immunocompetent mice. *Gene Ther.* **6**, 1751–1758 (1999).
- Polack, F. P. et al. Safety and efficacy of the BNT162b2 mRNA Covid-19 vaccine. *N. Engl. J. Med.* **383**, 2603–2615 (2020).
- Dario, A. & Tomei, G. The safety of the temozolomide in patients with malignant glioma. *Curr. Drug Saf.* **1**, 205–222 (2006).
- Coutinho, A. E. & Chapman, K. E. The anti-inflammatory and immunosuppressive effects of glucocorticoids, recent developments and mechanistic insights. *Mol. Cell. Endocrinol.* **335**, 2–13 (2011).
- Desjardins, A. et al. Recurrent glioblastoma treated with recombinant poliovirus. *N. Engl. J. Med.* **379**, 150–161 (2018).

25. Markert, J. M. et al. Conditionally replicating herpes simplex virus mutant, G207 for the treatment of malignant glioma: results of a phase I trial. *Gene Ther.* **7**, 867–874 (2000).
26. Markert, J. M. et al. Phase Ib trial of mutant herpes simplex virus G207 inoculated pre- and post-tumor resection for recurrent GBM. *Mol. Ther.* **17**, 199–207 (2009).
27. Markert, J. M. et al. A phase I trial of oncolytic HSV-1, G207, given in combination with radiation for recurrent GBM demonstrates safety and radiographic responses. *Mol. Ther.* **22**, 1048–1055 (2014).
28. Todo, T., Rabkin, S. D., Chahlavi, A. & Martuza, R. L. Corticosteroid administration does not affect viral oncolytic activity, but inhibits antitumor immunity in replication-competent herpes simplex virus tumor therapy. *Hum. Gene Ther.* **10**, 2869–2878 (1999).
29. Van Gool, F. et al. A mutation in the transcription factor Foxp3 drives T helper 2 effector function in regulatory T cells. *Immunity* **50**, 362–377.e366 (2019).
30. Andtbacka, R. H. I. et al. Final analyses of OPTiM: a randomized phase III trial of talimogene laherparepvec versus granulocyte-macrophage colony-stimulating factor in unresectable stage III–IV melanoma. *J. Immunother. Cancer* **7**, 145 (2019).
31. Aghi, M., Rabkin, S. D. & Martuza, R. L. Angiogenic response caused by oncolytic herpes simplex virus-induced reduced thrombospondin expression can be prevented by specific viral mutations or by administering a thrombospondin-derived peptide. *Cancer Res.* **67**, 440–444 (2007).
32. Carpenter, A. B., Carpenter, A. M., Aiken, R. & Hanft, S. Oncolytic virus in gliomas: a review of human clinical investigations. *Ann. Oncol.* **32**, 968–982 (2021).
33. Lang, F. F. et al. Phase I study of DNX-2401 (Delta-24-RGD) oncolytic adenovirus: replication and immunotherapeutic effects in recurrent malignant glioma. *J. Clin. Oncol.* **36**, 1419–1427 (2018).
34. Friedman, G. K. et al. Oncolytic HSV-1 G207 immunovirotherapy for pediatric high-grade gliomas. *N. Engl. J. Med.* **384**, 1613–1622 (2021).
35. Fukuhara, H., Ino, Y. & Todo, T. Oncolytic virus therapy: a new era of cancer treatment at dawn. *Cancer Sci.* **107**, 1373–1379 (2016).
36. Fukuhara, H., Martuza, R. L., Rabkin, S. D., Ito, Y. & Todo, T. Oncolytic herpes simplex virus vector G47Δ in combination with androgen ablation for the treatment of human prostate adenocarcinoma. *Clin. Cancer Res.* **11**, 7886–7890 (2005).
37. Sugawara, K. et al. Efficacy of a third-generation oncolytic herpes virus G47Δ in advanced stage models of human gastric cancer. *Mol. Ther. Oncolytics* **17**, 205–215 (2020).
38. Yamada, T., Tateishi, R., Iwai, M., Koike, K. & Todo, T. Neoadjuvant use of oncolytic herpes virus G47Δ enhances the antitumor efficacy of radiofrequency ablation. *Mol. Ther. Oncolytics* **18**, 535–545 (2020).
39. Liu, R., Martuza, R. L. & Rabkin, S. D. Intracarotid delivery of oncolytic HSV vector G47Δ to metastatic breast cancer in the brain. *Gene Ther.* **12**, 647–654 (2005).
40. Uchihashi, T. et al. Oncolytic herpes virus G47Δ injected into tongue cancer swiftly traffics in lymphatics and suppresses metastasis. *Mol. Ther. Oncolytics* **22**, 388–398 (2021).
41. Yajima, S. et al. Efficacy and safety of a third-generation oncolytic herpes virus G47Δ in models of human esophageal carcinoma. *Mol. Ther. Oncolytics* **23**, 402–411 (2021).
42. Wu, A. et al. Biological purging of breast cancer cells using an attenuated replication-competent herpes simplex virus in human hematopoietic stem cell transplantation. *Cancer Res.* **61**, 3009–3015 (2001).
43. Ishino, R. et al. Oncolytic virus therapy with HSV-1 for hematological malignancies. *Mol. Ther.* **29**, 762–774 (2021).
44. Oku, M. et al. Oncolytic herpes simplex virus type 1 (HSV-1) in combination with lenalidomide for plasma cell neoplasms. *Br. J. Haematol.* **192**, 343–353 (2021).
45. Saha, D., Martuza, R. & Rabkin, S. Abstract B116: Immunovirotherapy in combination with immune checkpoint inhibitors for treating glioblastoma. *Cancer Immunol. Res.* **4**, B116–B116 (2016).
46. Sugawara, K. et al. Oncolytic herpes virus G47Δ works synergistically with CTLA-4 inhibition through dynamic intratumoral immune modulation. *Mol. Ther. Oncolytics* **22**, 129–142 (2021).

Publisher's note Springer Nature remains neutral with regard to jurisdictional claims in published maps and institutional affiliations.



Open Access This article is licensed under a Creative Commons Attribution 4.0 International License, which permits use, sharing, adaptation, distribution and reproduction in any medium or format, as long as you give appropriate credit to the original author(s) and the source, provide a link to the Creative Commons license, and indicate if changes were made. The images or other third party material in this article are included in the article's Creative Commons license, unless indicated otherwise in a credit line to the material. If material is not included in the article's Creative Commons license and your intended use is not permitted by statutory regulation or exceeds the permitted use, you will need to obtain permission directly from the copyright holder. To view a copy of this license, visit <http://creativecommons.org/licenses/by/4.0/>.

© The Author(s) 2022

Methods

Study design and participants. This investigator-initiated phase 2 trial was conducted at a single institution (the Institute of Medical Science Hospital, the University of Tokyo (IMSUT Hospital)) in Japan (UMIN-CTR Clinical Trial Registry, UMIN000015995, registered and posted on 18 December 2014). The first patient enrollment date was 19 May 2015 and the last patient enrollment date was 18 April 2018. This study was approved by the PMDA on 29 August 2014. Under the guidance of the PMDA, it was recommended that this study be conducted at a single institution for safety reasons, as this was the first PMDA-supervised clinical trial of oncolytic virus therapy. The data cut-off date for the Case Study Report submitted to the PMDA was 6 April 2020, although survival-related data continued to be collected until 1 March 2022 and are presented here.

The full inclusion and exclusion criteria are listed below.

Inclusion criteria:

- (i) age 18 yr or older
- (ii) a pathologically confirmed diagnosis of glioblastoma with a persistent or recurrent tumor (represented as a contrast-enhanced lesion of ≥ 1.0 cm on MRI) despite having received radiation therapy and temozolomide
- (iii) a Karnofsky Performance Scale score $\geq 60\%$
- (iv) a constant steroid dosage within 1 week on the day of eligibility assessment
- (v) able to use barrier-type contraceptive during the study and for 6 months after the last dose of drug
- (vi) potential to survive ≥ 3 months
- (vii) laboratory data meet the following criteria (white blood cell count $> 2,000$ per mm^3 , neutrophil count $> 1,000$ per mm^3 , platelet count $> 100,000$ per mm^3 , haemoglobin level > 9.0 g dl^{-1} , prothrombin time-international normalized ratio (PT-INR) ≤ 1.3 times the upper limit of the institution baseline, serum creatinine < 1.7 mg dl^{-1} , aspartate aminotransferase (AST) and alanine aminotransferase (ALT) ≤ 4 times the upper limit of the institution baseline, total bilirubin or direct bilirubin ≤ 1.5 mg dl^{-1}).

Exclusion criteria:

- (i) confirmed presence of any of the following tumors: metastatic tumors outside of the brain; multiple intracranial malignant glioma lesions (considered as multiple contrast-enhanced lesions with separate Fluid Attenuated Inversion Recovery (FLAIR) high-intensity areas); tumors located in the ventricles, brainstem or posterior fossa; or tumors for which the investigational product (G47 Δ) must be administered via the ventricles, subependymal or subarachnoidal dissemination
- (ii) past or current medical history of any of the following: encephalitis, multiple sclerosis or other central nervous system infections; positive for human immunodeficiency virus; or conditions in which the use of MRI contrast media is contraindicated (for example, patients with a pacemaker or continuous infusion pump in the body or patients allergic to MRI contrast media)
- (iii) any of the following complications: active herpes virus infection; herpes virus infections requiring treatment with an antiviral (acyclovir or valacyclovir); active, poorly controlled infection that prevents surgery; uncontrolled or severe heart failure; diabetes mellitus; hypertension; interstitial pneumonia; renal failure; autoimmune disease; addiction to alcohol or other drugs; other active malignancies
- (iv) history of allergy to antivirals (acyclovir or valacyclovir)
- (v) history of receiving any of the following treatments or operations: other investigational products or investigational therapies (within 30 d before G47 Δ administration, or within 5 times the half-life of other investigational products or investigational therapies, whichever is longer); brain tumor resection (within 30 d before G47 Δ administration); gene therapy or oncolytic virus therapy other than G47 Δ ; bevacizumab (within 30 d before G47 Δ administration)
- (vi) pregnancy or lactation
- (vii) otherwise considered ineligible for inclusion by the principal investigator or the subinvestigator

In the above exclusion criteria, multiple contrast-enhanced lesions with separate Fluid Attenuated Inversion Recovery (FLAIR) high-intensity areas were considered as multiple intracranial malignant glioma lesions.

All patients enrolled in the trial provided written, informed consent. The protocol was approved by the institutional review board of the Institution of Medical Science, the University of Tokyo. Patients were not compensated for trial participation.

Because of the unprecedented administration route of this anti-cancer drug, an intratumoral injection via stereotactic surgery, it was discussed and agreed with the PMDA to target a glioblastoma lesion that was either residual or recurrent, since such was likely to be the disease indication upon drug approval. To minimize a one-institution study bias, all consecutive patients that met the criteria were included in the order registered without exception. All histology specimens used for diagnosis of enrolled patients were reviewed by a neuropathologist on our team to confirm the diagnosis of glioblastoma.

MGMT methylation status was provided from referring hospitals for five patients. IDH1 mutation status and MGMT expression were tested post hoc by

immunohistochemistry using paraffin-embedded formalin-fixed slide sections of the initial surgery provided by referring hospitals. Primary antibodies for IDH1 mutation (R132H) and MGMT were anti-IDH1 R132H/DIA-H09 Mouse monoclonal anti-brain tumor marker Clone H09 (Dianova; DIA-H09) and anti-MGMT antibody [MT3.1] (Abcam; ab39253), respectively.

G47 Δ formulation. Test products were prepared at the Therapeutic Vectors Development Center, IMSUT Hospital, and consisted of G47 Δ suspended in 10% glycerol/phosphate buffer solution. Formulations were dispensed and stored in polypropylene cryotubes at -80°C . Before surgery, G47 Δ was adjusted to a concentration of 1×10^9 p.f.u. ml^{-1} and kept on ice until use. The titer of the original stock used in this trial was 1.2×10^{10} p.f.u. ml^{-1} . The clinical lot was tested for stability by titration at sequential time points, which showed that the virus titer of the product was stable for at least 7 d at room temperature and for approximately 2 months at 4°C . The time from thawing to injection ranged from 1 to 3 h approximately.

Intervention. G47 Δ was administered intratumorally by MRI-guided stereotactic surgery at intervals of 5–14 d for the first and second doses, and up to six doses at intervals of 4 ± 2 weeks for the third and subsequent doses. A total of 1×10^9 p.f.u. per dose in 1 ml of solution was divided equally and injected into 1–3 coordinates within a tumor using the Biopsy/Injection Needle (MES-CG07-200-01, Mizuho). This Biopsy/Injection Needle device was specifically designed for oncolytic virus injection, so that there is little dead space (15 μl) between the attached syringe and the injection needle exit. The device consists of an outer guide (outer cylinder), a biopsy needle and an injection needle, and either of the latter two needles can be inserted into the outer guide without moving the position of the guide. Therefore, the coordinates of biopsy and G47 Δ injection were exactly the same. Biopsy always preceded G47 Δ injection. G47 Δ was injected manually at a speed of 0.2 ml min^{-1} . After injection, the injection needle was kept in place for 5 min before retraction to avoid reflux. From the second dose onwards, G47 Δ was injected into viable tumor sites, depicted as contrast-enhanced portions on MRI, remaining from previous injections.

Radiation therapy was prohibited during the study. Steroid administration was permitted, but new doses or dose changes had to be recorded. Concomitant temozolomide was allowed, whereas other antineoplastic agents were prohibited.

The criteria for treatment discontinuation were as follows: (1) target lesion size < 1 cm; (2) progressive disease judgment under response criteria; (3) aggravation of clinical symptoms; (4) patient's wish to discontinue treatment or clinical judgment by the principal investigator or subinvestigator.

Outcomes. The primary endpoint was the 1-yr survival rate after G47 Δ treatment initiation. Secondary endpoints included OS and PFS after initial G47 Δ administration, tumor response for efficacy and adverse event frequency.

As one of the secondary endpoints, the best overall response during the observation period (2 yr after the last administration) was assessed by consecutive MRI assessments according to the response criteria adopted for this trial. These response criteria were designed for this clinical trial with reference to immune-related response criteria¹⁷ and approved by the PMDA. MRI data after administration of bevacizumab after disease progression were not used for the overall response rate evaluation.

The response criteria are as follows:

Complete response: two consecutive MRI scans performed at an interval of at least about 4 weeks show complete disappearance of a target lesion, with no appearance of new lesions.

Partial response: two consecutive MRI scans performed at an interval of at least about 4 weeks show a decrease in the sum of areas of target lesions by at least 50% compared with that before the first dose, with no appearance of new lesions.

Stable disease: response other than complete response, partial response or progressive disease.

Progressive disease: two consecutive MRI scans performed at an interval of at least about 4 weeks show an increase in the sum of areas of target lesions by at least 25% compared with that on the respective last MRI scans, or appearance of new lesion(s).

Tumor cross-sectional area was defined as (the largest diameter) \times (the diameter perpendicular to the largest diameter) of the circumference of the contrast-enhanced lesion on an axial section of MRI.

Adverse events were classified and graded using the National Cancer Institute Common Terminology Criteria for Adverse Events (CTCAE v.4.03) terminology. Differentiation of adverse events caused by G47 Δ and those caused by surgical injection procedures was judged by the investigator (neurosurgeon).

Sample collection for viral shedding. For each patient, blood and urine samples were collected after G47 Δ administration on the same day (day 0); blood, urine and saliva samples on days 1, 2 and 3 for the first G47 Δ administration; and on days 1, 2, 3 and 7 for the second G47 Δ administration onwards for every administration.

Statistical planning and interim analysis. At planning, this trial assumed achievement of a 1-yr survival rate of 40% based on the results of the

FIH trial³. Based on the 1-yr survival rate for recurrent glioblastoma after chemo-radiotherapy (14%)³, the comparative control value was set to 15%. Assuming a superiority of G47Δ of 5% on one side and a power of 80%, and one interim analysis to be performed, the treatment arm size was calculated as 25 patients. An interim analysis was to be conducted when the number of patients followed for 1 yr from the initiation of study treatment reached 13 patients, so the study was designed to include 30 patients to ensure adequate enrollment. The increase in the number of Type I errors resulting from the interim analysis will be adjusted by the Lan–Demet method using the O’Brien–Fleming type α . The significance level of the hypothesis test will be set at 0.557% on one side. Efficacy and safety analyses included all patients who received at least one dose of G47Δ, and this defined the FAS for efficacy and the safety analysis set for safety.

Statistical analysis. Patient background factors were aggregated according to the characteristics of the data. For the primary endpoint, a 1-yr survival rate after G47Δ initiation was calculated along with the 95% CI. For the secondary endpoints, an OS after G47Δ initiation, a PFS after G47Δ initiation and an OS from the initial surgery with respective 95% CIs were calculated by the Kaplan–Meier method. Adverse events for the safety assessment were analyzed by event. Data analyses were done with SAS Windows, v.9.4 (SAS Institute), or IBM SPSS Statistics v.22 software (IBM Corporation). For the survival data, 30 d were calculated as 1 month according to the Clinical Study Report submitted to the PMDA.

Reporting summary. Further information on research design is available in the Nature Research Reporting Summary linked to this article.

Data availability

Any requests for raw and analyzed data will be reviewed by the Institute of Medical Science Hospital, the University of Tokyo. Patient-related data not included in the paper were generated as part of a clinical trial and are subject to patient confidentiality. Any data and materials (for example, tissue samples or imaging data) that can be shared will need approval from the Institute of Medical Science Hospital, the University of Tokyo. Any data shared will be de-identified. Requests should be made to the corresponding author (toudou-nsu@umin.ac.jp); response time will be within approximately 5–10 business days. Source data are provided with this paper.

References

47. Wolchok, J. D. et al. Guidelines for the evaluation of immune therapy activity in solid tumors: immune-related response criteria. *Clin. Cancer Res.* **15**, 7412–7420 (2009).

Acknowledgements

We thank M. Iwai, S. Kanayama, H. Momota, L. Chalise, K. Saiga, E. Ozaki and the members of the Division of Innovative Cancer Therapy, the members of the Therapeutic Vector Development Center and the staff of the Center for Translational Research, the Institute of Medical Science, the University of Tokyo, for their support and assistance in carrying out this clinical study. We also thank R. Nishikawa (Saitama Medical University), S. Aoki (Juntendo University) and K. Yoshimura (Kanazawa University) for serving the Independent Data Monitoring Committee, and Y. Furukawa (the University of Tokyo) for helping us with the genome sequencing of G47Δ. This research was supported in part by the Japanese Agency for Medical Research and Development (AMED) ‘Innovative Cancer Medical Practical Research Project’ (2015–2020) under grant nos. JP15ck0106144 and JP18ck0106416 and ‘Translational Research Program’ under grant no. JP20lm0203140 to T.T. We thank Y. Okamoto and M. Snape of inScience Communications, Springer Healthcare, for helping us write the first draft of the manuscript. This medical writing assistance was funded by the Division of Innovative Cancer Therapy, the Institute of Medical Science, the University of Tokyo.

Author contributions

T.T. is the principal investigator of the study. T.T. performed supervision, investigation, data curation, data analysis, interpretation and writing and is responsible for methodology and funding acquisition. H.L., Y.I. and M.T. performed investigation and data curation. M.T. also performed data analysis and writing. H.O. is responsible for data curation and statistical analysis. Y.O. and J.S. are responsible for pathological analysis. All authors approved the final version of this manuscript and are accountable for all aspects of the work.

Competing interests

T.T. owns the patent right for G47Δ in Japan. All other authors have no conflict of interest to declare.

Additional information

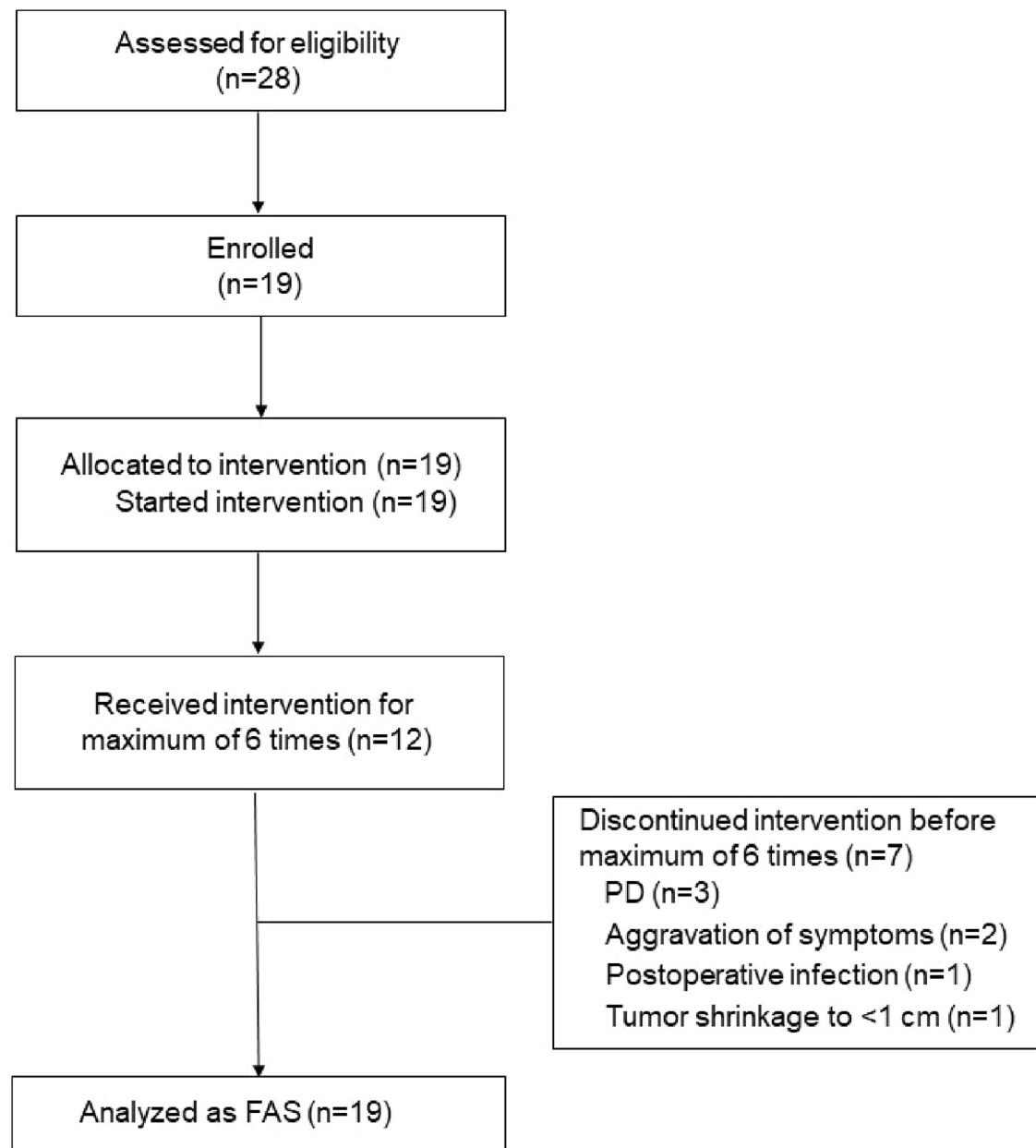
Extended data is available for this paper at <https://doi.org/10.1038/s41591-022-01897-x>.

Supplementary information The online version contains supplementary material available at <https://doi.org/10.1038/s41591-022-01897-x>.

Correspondence and requests for materials should be addressed to Tomoki Todo.

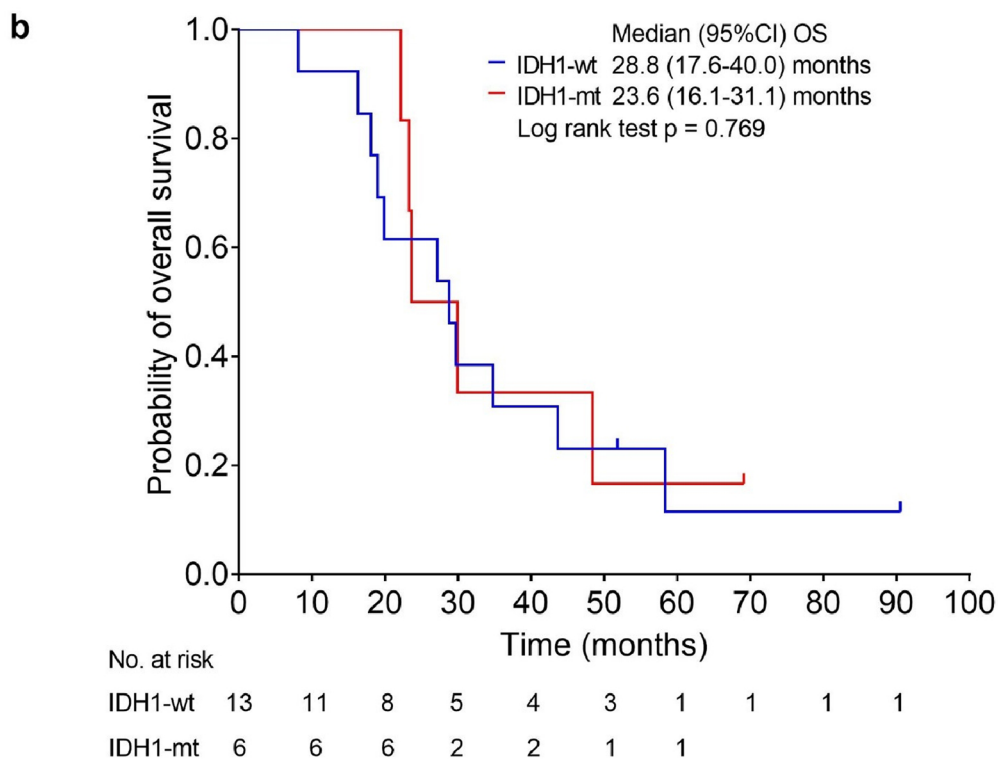
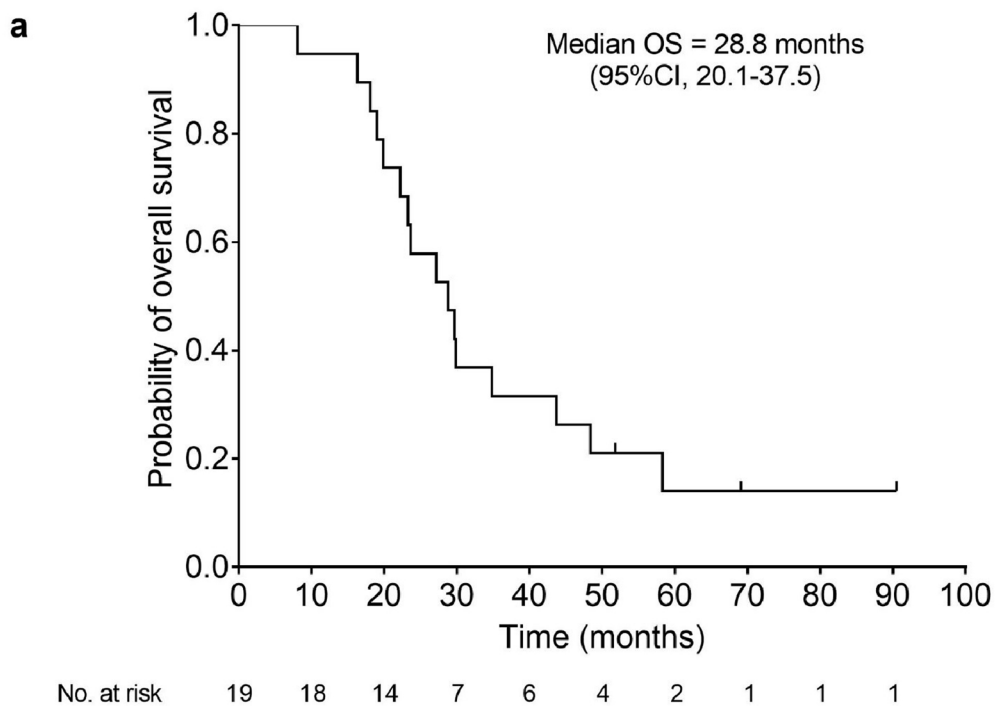
Peer review information *Nature Medicine* thanks the anonymous reviewers for their contribution to the peer review of this work. Primary Handling Editors: Saheli Sadanand and Anna Maria Ranzoni, in collaboration with the *Nature Medicine* team.

Reprints and permissions information is available at www.nature.com/reprints.



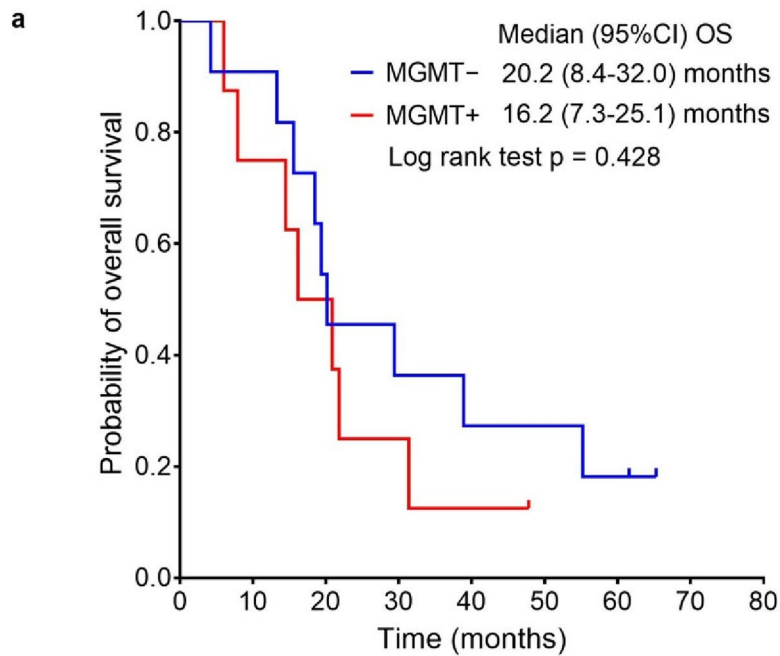
Extended Data Fig. 1 | Patient disposition. Of 28 patients who gave informed consent, 19 patients who matched the eligibility criteria were enrolled and composed the full analysis set (FAS).

a Overall survival from the initial surgery. **b** Overall survival based on IDH1 status from the initial surgery.

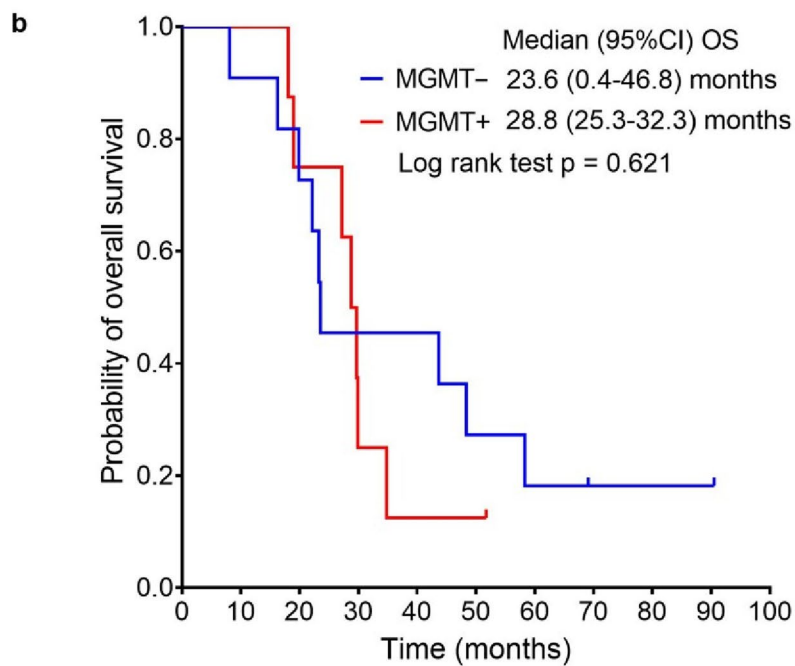


Extended Data Fig. 2 | Kaplan-Meier curves from the initial surgery. a Overall survival from the initial surgery. **b** Overall survival based on IDH1 status from the initial surgery.

a Overall survival after G47 Δ initiation. **b** Overall survival from the initial surgery.

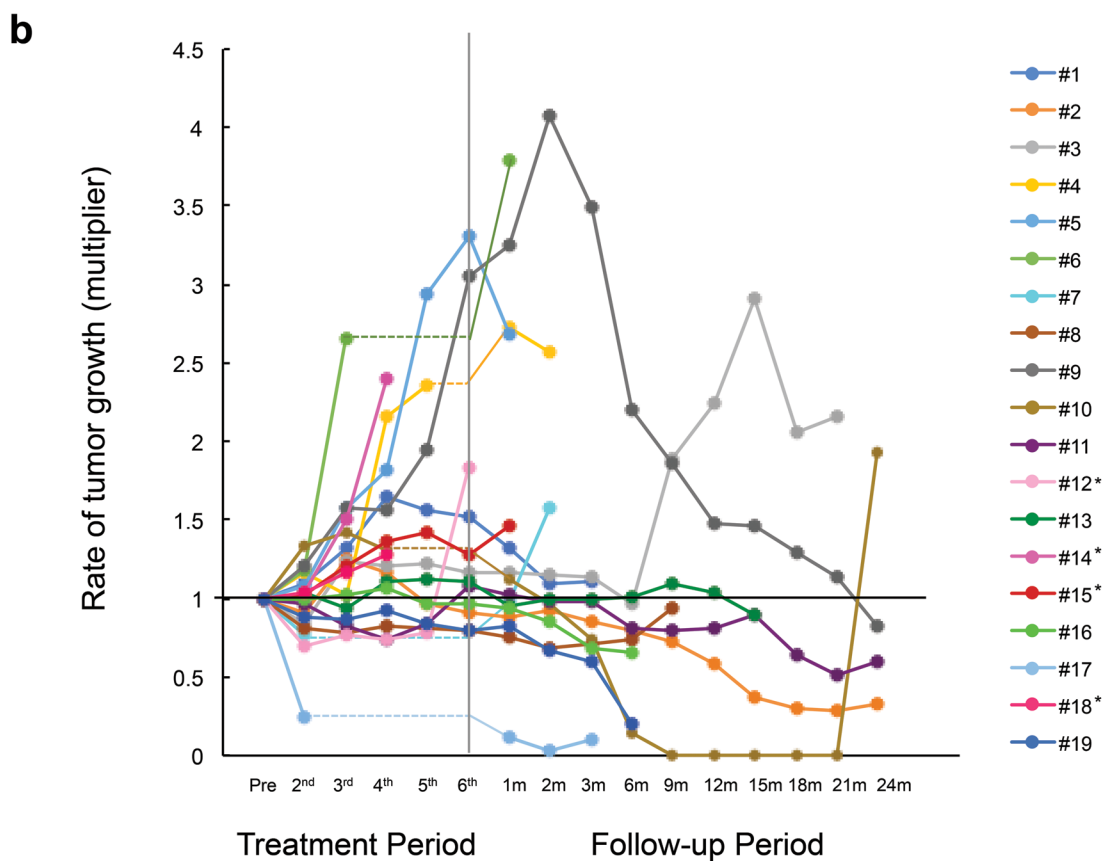
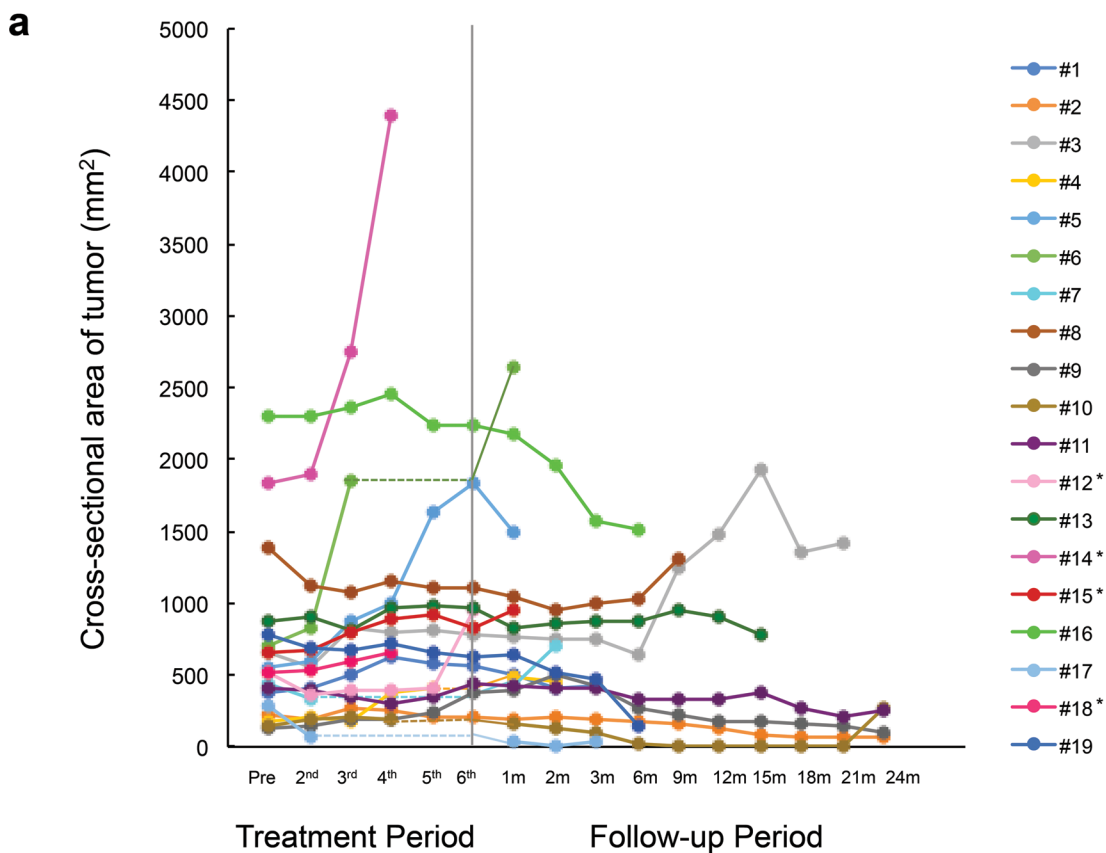


No. at risk							
MGMT-	11	10	6	4	3	3	2
MGMT+	8	6	4	2	1		



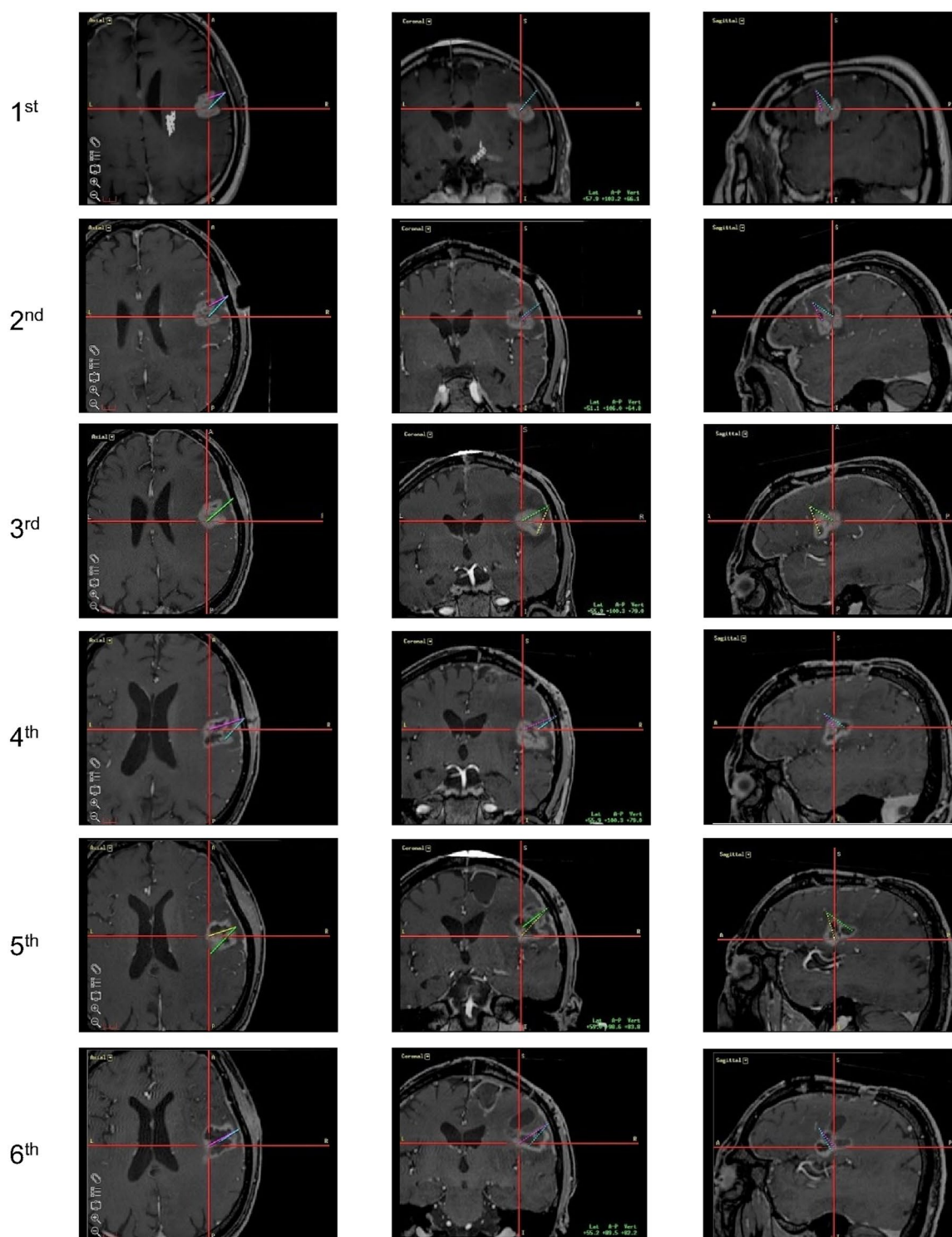
No. at risk										
MGMT-	11	10	8	5	5	3	2	1	1	1
MGMT+	8	8	6	2	1	1				

Extended Data Fig. 3 | Kaplan-Meier curves based on MGMT expression. **a** Overall survival after G47 Δ initiation. **b** Overall survival from the initial surgery.

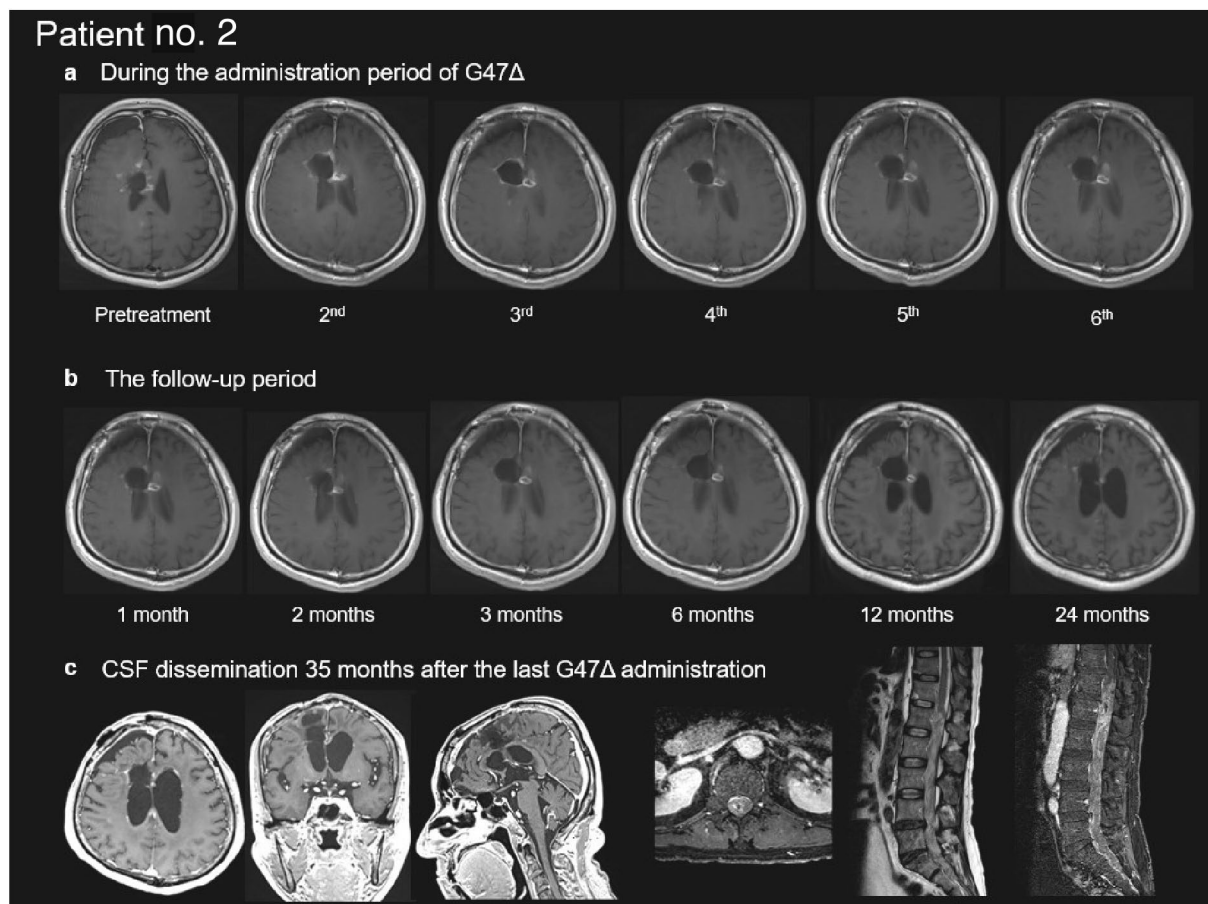


Extended Data Fig. 4 | See next page for caption.

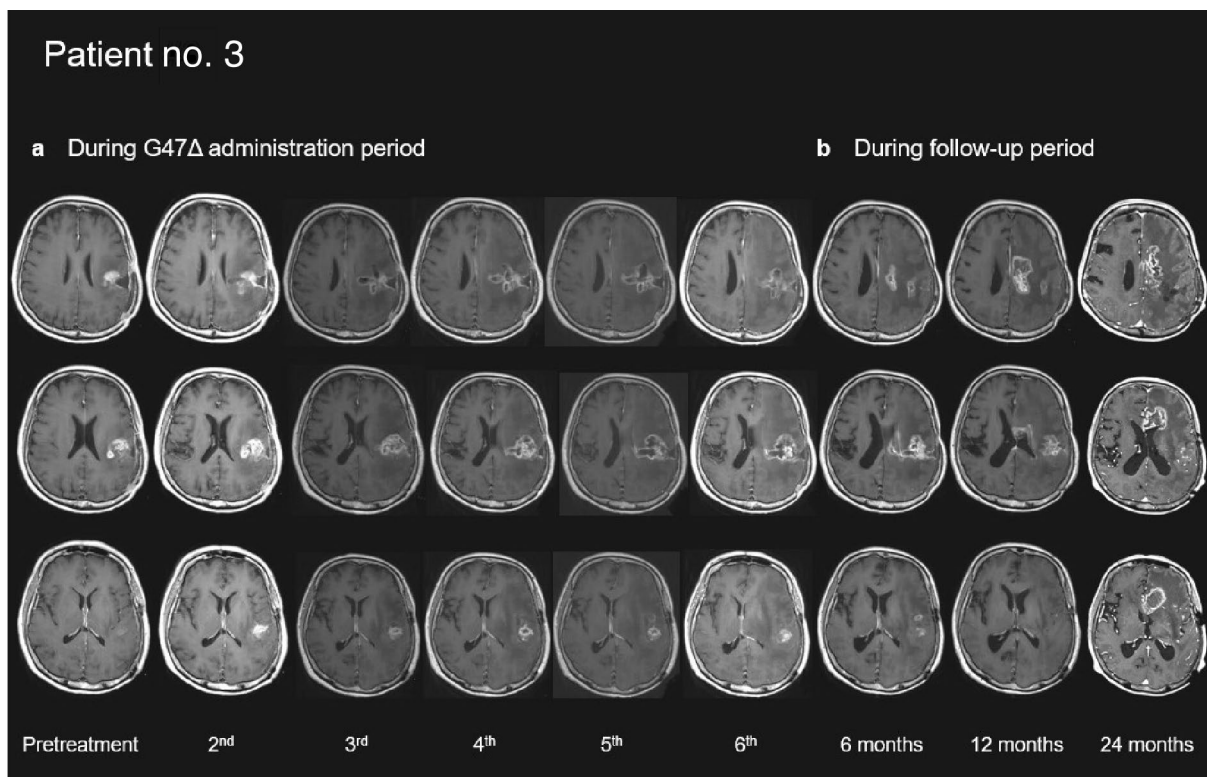
Extended Data Fig. 4 | Time course of cross-sectional area of the target lesion of individual patients. **a** Cross-sectional area (CSA) of the target lesion expressed as actual area at every assessment point. The median CSA of the tumor at baseline was 519.9 mm² (range, 122.4-2,306.7 mm²). **b** CSA of the target lesion expressed as a ratio relative to the pre-treatment area. The target lesions tended to show a temporary increase in area during G47Δ treatment. Twelve patients (63.2%) showed a decrease in target lesion area for a certain time compared to pre-treatment. In patients who did not receive G47Δ for the maximum of 6 times, the period during which they were not administered is expressed as a horizontal dotted line. * indicates patients who received corticosteroids.



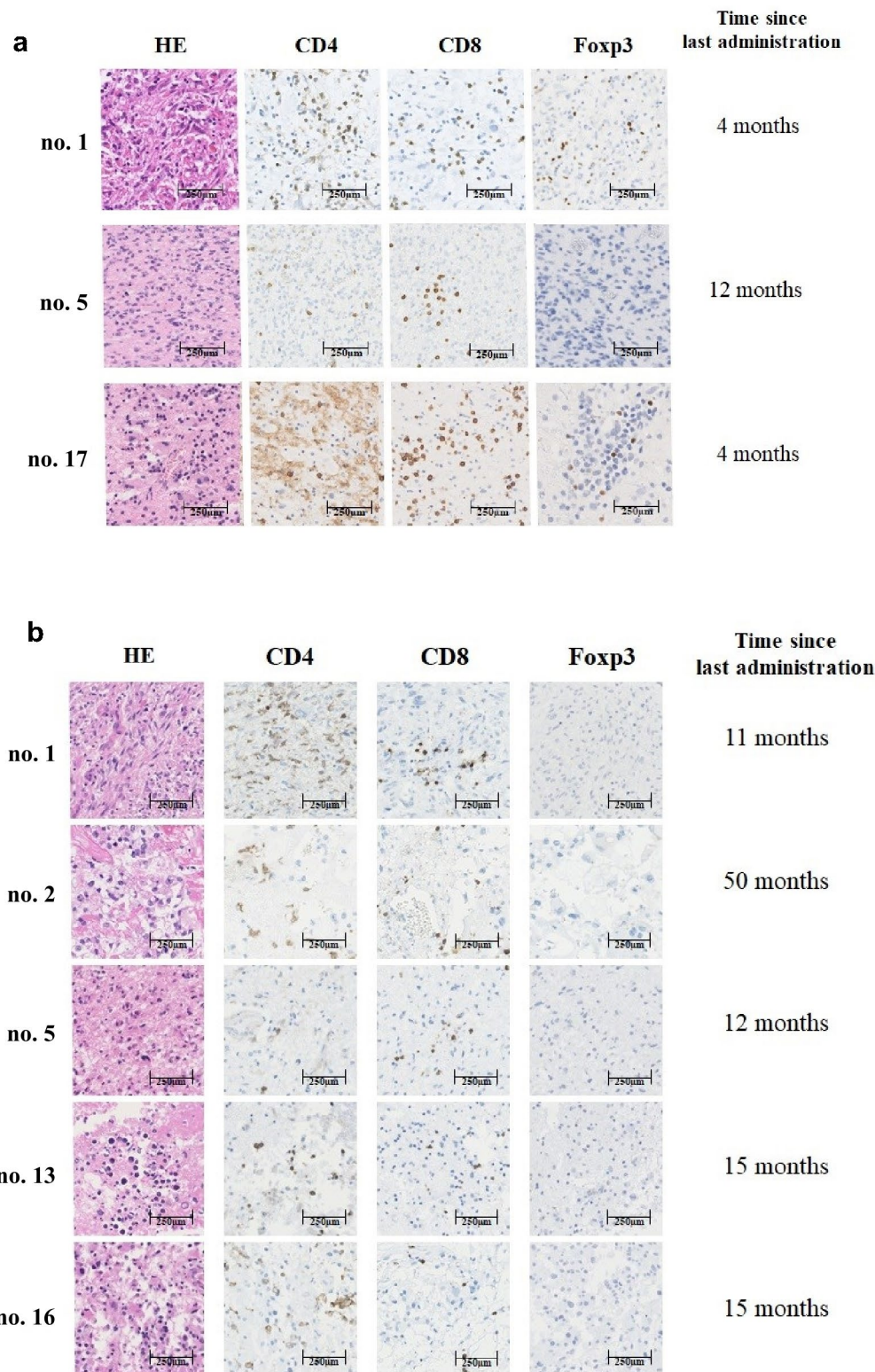
Extended Data Fig. 5 | Planning MRI of a representative case (patient no. 1). Individual planning MRI of patient no. 1 using StealthStation Surgical Navigation System from the 1st to the 6th dose displaying 2 administration routes for each dose. Axial (left), coronal (middle) and sagittal (right) sections are shown for each dose. G47 Δ was injected into viable tumor sites, depicted as contrast-enhanced portions on MRI, remaining from previous injections.



Extended Data Fig. 6 | Representative case (patient no. 2) showing cerebrospinal fluid dissemination at progression. a Characteristic MRI changes are observed with an overall lesion size increased during the administration period. **b** Shrinkage of the target lesion is observed at 12 months after the last G47 Δ administration. **c** Cerebrospinal fluid (CSF) dissemination is observed in the brain and in the spinal cord at 35 months after the last G47 Δ administration. Note that the target lesion is well controlled. The disease course since the initiation of G47 Δ therapy was 55.2 months.



Extended Data Fig. 7 | Representative case (patient no. 3) showing target lesion shrinkage and subsequent progression adjacent to but away from G47 Δ injected sites. **a Characteristic MRI changes are observed, resulting in a large clearing area within, and an enlargement of, the target lesion. **b** The target lesion is reduced in size at 6 months after the last G47 Δ administration. At 12 months, while the target lesion keeps shrinking, a progression is seen in the brain adjacent to the target lesion anterior-medially. The progression continues at 24 months. The disease course since the initiation of G47 Δ therapy was 31.4 months.**



Extended Data Fig. 8 | Histology of regrown tumors at reoperation and brain lesions at autopsy. a After G47 Δ therapy, 3 patients underwent craniotomy for tumor resection of regrown tumors (no. 1 and no. 17 at 4 months and no. 5 at 12 months after the last G47 Δ administration). Infiltrating numbers of CD4+ and CD8+ lymphocytes remained abundantly increased in the two cases at 4 months and to some extent in the case at 12 months. Increased numbers of Foxp3+ cells were found in the two cases at 4 months and both underwent reoperation, but not found in the case at 12 months. Each is representative of 3 tissue samples. **b** Among 5 patients who underwent autopsy, 4 patients died of tumor progression (no. 1, no. 2, no. 5 and no. 16) and an infiltration of CD4+ and CD8+ lymphocytes and a low number of Foxp3+ cells persisted at autopsy 11 to 50 months after the last G47 Δ administration. In patient no. 13 whose target lesion was well controlled at the time of death, necrosis and calcification, but no viable tumor cells, were found in the brain at autopsy 15 months after the last G47 Δ administration. Each is representative of 3 tissue samples.

Reporting Summary

Nature Research wishes to improve the reproducibility of the work that we publish. This form provides structure for consistency and transparency in reporting. For further information on Nature Research policies, see our [Editorial Policies](#) and the [Editorial Policy Checklist](#).

Statistics

For all statistical analyses, confirm that the following items are present in the figure legend, table legend, main text, or Methods section.

n/a Confirmed

- The exact sample size (n) for each experimental group/condition, given as a discrete number and unit of measurement
- A statement on whether measurements were taken from distinct samples or whether the same sample was measured repeatedly
- The statistical test(s) used AND whether they are one- or two-sided
Only common tests should be described solely by name; describe more complex techniques in the Methods section.
- A description of all covariates tested
- A description of any assumptions or corrections, such as tests of normality and adjustment for multiple comparisons
- A full description of the statistical parameters including central tendency (e.g. means) or other basic estimates (e.g. regression coefficient) AND variation (e.g. standard deviation) or associated estimates of uncertainty (e.g. confidence intervals)
- For null hypothesis testing, the test statistic (e.g. F , t , r) with confidence intervals, effect sizes, degrees of freedom and P value noted
Give P values as exact values whenever suitable.
- For Bayesian analysis, information on the choice of priors and Markov chain Monte Carlo settings
- For hierarchical and complex designs, identification of the appropriate level for tests and full reporting of outcomes
- Estimates of effect sizes (e.g. Cohen's d , Pearson's r), indicating how they were calculated

Our web collection on [statistics for biologists](#) contains articles on many of the points above.

Software and code

Policy information about [availability of computer code](#)

Data collection SAS Windows, version 9.4 (SAS Institute Inc., Cary, NC, USA)

Data analysis IBM SPSS Statistics version 22 software (IBM Corporation, Somers, USA)

For manuscripts utilizing custom algorithms or software that are central to the research but not yet described in published literature, software must be made available to editors and reviewers. We strongly encourage code deposition in a community repository (e.g. GitHub). See the Nature Research [guidelines for submitting code & software](#) for further information.

Data

Policy information about [availability of data](#)

All manuscripts must include a [data availability statement](#). This statement should provide the following information, where applicable:

- Accession codes, unique identifiers, or web links for publicly available datasets
- A list of figures that have associated raw data
- A description of any restrictions on data availability

Any requests for raw and analyzed data will be reviewed by the Institute of Medical Science Hospital, the University of Tokyo. Patient-related data not included in the paper were generated as part of a clinical trial and are subject to patient confidentiality. Any data and materials (for example, tissue samples or imaging data) that can be shared will need approval from the Institute of Medical Science Hospital, the University of Tokyo. Any data shared will be de-identified. Requests should be made to Tomoki Todo (toudou-nsu@umin.ac.jp); response time will be within approximately 5-10 business days.

Field-specific reporting

Please select the one below that is the best fit for your research. If you are not sure, read the appropriate sections before making your selection.

Life sciences Behavioural & social sciences Ecological, evolutionary & environmental sciences

For a reference copy of the document with all sections, see [nature.com/documents/nr-reporting-summary-flat.pdf](https://www.nature.com/documents/nr-reporting-summary-flat.pdf)

Life sciences study design

All studies must disclose on these points even when the disclosure is negative.

Sample size	At planning, this trial assumed achievement of a 1-year survival rate of 40% based on the results of the FIH trial ² . Based on the 1-year survival rate for recurrent glioblastoma after chemo-radiotherapy (14%) ³ , the comparative control value was set to 15%. Assuming a superiority of G47Δ of 5% on one side and a power of 80%, and one interim analysis to be performed, the treatment arm size was calculated as 25 patients. An interim analysis was to be conducted when the number of patients followed for 1 year from the initiation of study treatment reached 13 patients, so the study was designed to include 30 patients to ensure adequate enrollment. The increase in the number of Type I errors resulting from the interim analysis will be adjusted by the Lan-Demet's method using the O'Brien Fleming type α . The significance level of the hypothesis test will be set at 0.557% on one side. Efficacy and safety analyses included all patients who received at least one dose of G47Δ and this defined the full analysis set (FAS) for efficacy and the safety analysis set (SAS) for safety.
Data exclusions	Patients were excluded based on a priori criteria before the start of the study. There were no data excluded for enrolled patients.
Replication	Findings were from a cohort of patients with glioblastoma, all but 3 of whom are now deceased; replication in this cohort is therefore impossible.
Randomization	This was a phase II open-label study without randomization. Randomization was not feasible due to the nature of the surgical intervention and ethical restrictions related to 'sham' surgery in Japan.
Blinding	Blinding not conducted. Open-label study design using surgical patients made blinding not relevant.

Reporting for specific materials, systems and methods

We require information from authors about some types of materials, experimental systems and methods used in many studies. Here, indicate whether each material, system or method listed is relevant to your study. If you are not sure if a list item applies to your research, read the appropriate section before selecting a response.

Materials & experimental systems

n/a	Involved in the study
<input type="checkbox"/>	<input checked="" type="checkbox"/> Antibodies
<input checked="" type="checkbox"/>	<input type="checkbox"/> Eukaryotic cell lines
<input checked="" type="checkbox"/>	<input type="checkbox"/> Palaeontology and archaeology
<input checked="" type="checkbox"/>	<input type="checkbox"/> Animals and other organisms
<input type="checkbox"/>	<input checked="" type="checkbox"/> Human research participants
<input type="checkbox"/>	<input checked="" type="checkbox"/> Clinical data
<input checked="" type="checkbox"/>	<input type="checkbox"/> Dual use research of concern

Methods

n/a	Involved in the study
<input checked="" type="checkbox"/>	<input type="checkbox"/> ChIP-seq
<input checked="" type="checkbox"/>	<input type="checkbox"/> Flow cytometry
<input type="checkbox"/>	<input checked="" type="checkbox"/> MRI-based neuroimaging

Antibodies

Antibodies used

Antibodies used
 Anti-CD4 (rabbit) (clone EPR6855, Abcam, Cat. ab133616, Lot. GR3276764-5, dilution 1:250)
 Anti-CD8 (rabbit) (clone SP16, Abcam, Cat. ab101500, Lot. 9116S1711F, dilution 1:100)
 Anti-FoxP3 (rabbit) (clone SP97, Abcam, Cat. ab99963, Lot. GR3281127-15, dilution 1:50)
 Anti-HSV-1 (rabbit) (polyclonal, Gene Tex, Cat. GTX73373, Lot. 822100458, ready-to-use)
 Anti-IDH1 R132H (mouse) (clone H09, Dianova, Cat. DIA-H09, Lot. 211129/02, dilution 1:100)
 Anti-MGMT (mouse) (clone MT3.1, Abcam, Cat. ab39253, Lot. GR3422909-2, dilution 1:100)

Validation

All antibodies were purchased directly from manufacturers and the validation statements are available on website of the manufacturers. The application of all antibodies followed by the instructions of the website.
 Anti-CD4 (ab133616): <https://www.abcam.com/cd4-antibody-epr6855-ab133616.html>
 Anti-CD8 (ab101500): <https://www.abcam.com/cd8-alpha-antibody-sp16-ab101500.html>
 Anti-FoxP3 (ab99963): <https://www.abcam.com/foxp3-antibody-sp97-ab99963.html>
 Anti-HSV-1 (GTX73373): <https://www.genetex.com/Product/Detail/HSV1-antibody-ready-to-use/GTX73373>
 Anti-IDH1 R132H (DIA-H09): <https://www.dianova.com/en/shop/dia-h09-anti-idh1-r132h-hu-from-mouse-h09-unconj/>

Human research participants

Policy information about [studies involving human research participants](#)

Population characteristics	A total of 19 patients were included in the study who were diagnosed with residual or recurrent glioblastoma. Covariate-related characteristics of the 19 patients are included in Table 1.
Recruitment	Study participants were enrolled through patient referrals or the website of the Institute of Medical Science Hospital, the University of Tokyo. All eligible patients were enrolled sequentially without exception and intentional selection.
Ethics oversight	All patients enrolled in the trial provided written informed consent. The protocol was approved by the institutional review board of the Institution of Medical Science, the University of Tokyo. Patients were not compensated for trial participation.

Note that full information on the approval of the study protocol must also be provided in the manuscript.

Clinical data

Policy information about [clinical studies](#)

All manuscripts should comply with the ICMJE [guidelines for publication of clinical research](#) and a completed [CONSORT checklist](#) must be included with all submissions.

Clinical trial registration	UMIN-CTR Clinical Trial registry (UMIN000015995)
Study protocol	Full trial protocol is provided in the Supplementary Materials accompanying the main manuscript.
Data collection	Data was collected from patients who underwent study interventions at a single institution (the Institute of Medical Science Hospital, the University of Tokyo [IMSUT Hospital]) in Japan. The first patient enrollment date was May 19, 2015 and the last patient enrollment date was April 18, 2018. This study was approved by the Japanese Pharmaceuticals and Medical Devices Agency (PMDA) on August 29, 2014. Under the guidance of PMDA, it was recommended that this study be conducted at a single institution for safety reasons, as this was the first PMDA-supervised clinical trial of oncolytic virus therapy. The data cutoff date for the Case Study Report submitted to PMDA was April 6, 2020, although survival-related data continued to be collected until March 1, 2022.
Outcomes	The primary endpoint was the 1-year survival rate after G47 Δ treatment initiation. For the primary endpoint, a 1-year survival rate after G47 Δ initiation was calculated along with the 95% confidence interval. Secondary endpoints included OS, progression-free survival (PFS), tumor response for efficacy and adverse event frequency. Further details are recorded in the main manuscript. For the secondary endpoints, an overall survival after G47 Δ initiation, a progression-free survival after G47 Δ initiation and an overall survival from the initial surgery with respective 95% confidence intervals were calculated by the Kaplan-Meier method. Adverse events for the safety assessment were analyzed by event.

Magnetic resonance imaging

Experimental design

Design type	MRI with contrast enhancement according to protocol schedules.
Design specifications	MRI with contrast enhancement according to protocol schedules.
Behavioral performance measures	This was not an fMRI study.

Acquisition

Imaging type(s)	Enhanced 3D-T1WI
Field strength	3 Tesla
Sequence & imaging parameters	Standard parameters of the radiology departments of the institutions.
Area of acquisition	Whole brain
Diffusion MRI	<input type="checkbox"/> Used <input checked="" type="checkbox"/> Not used

Preprocessing

Preprocessing software	No preprocessing was performed; MR images were directly analyzed in our PACS.
Normalization	N/A based on no preprocessing performed
Normalization template	N/A based on no preprocessing performed

Noise and artifact removal

Volume censoring

Statistical modeling & inference

Model type and settings

Effect(s) tested

Specify type of analysis: Whole brain ROI-based Both

Statistic type for inference
(See [Eklund et al. 2016](#))

Correction

Models & analysis

n/a | Involved in the study

Functional and/or effective connectivity

Graph analysis

Multivariate modeling or predictive analysis